

Robust Decentralized Navigation of Multi-Agent Systems with Collision Avoidance and Connectivity Maintenance Using Model Predictive Controllers

Alexandros Filotheou, Alexandros Nikou and Dimos V. Dimarogonas

The authors are with the KTH Center of Autonomous Systems and ACCESS Linnaeus Center, School of Electrical Engineering and Computer Science, KTH Royal Institute of Technology, SE-100 44, Stockholm, Sweden.

ARTICLE HISTORY

Compiled April 25, 2018

ABSTRACT

This paper addresses the problem of navigation control of a general class of 2nd order uncertain nonlinear multi-agent systems in a bounded workspace, which is a subset of \mathbb{R}^3 , with static obstacles. In particular, we propose a decentralized control protocol such that each agent reaches a predefined position at the workspace, while using local information based on a limited sensing radius. The proposed scheme guarantees that the initially connected agents remain always connected. In addition, by introducing certain distance constraints, we guarantee inter-agent collision avoidance as well as collision avoidance with the obstacles and the boundary of the workspace. The proposed controllers employ a class of Decentralized Nonlinear Model Predictive Controllers (DNMPC) under the presence of disturbances and uncertainties. Finally, simulation results verify the validity of the proposed framework.

KEYWORDS

Multi-Agent Systems; Decentralized Control; Nonlinear Model Predictive Control; Robust Control; Collision Avoidance.

1. Introduction

During the last decades, decentralized control of multi-agent systems has gained a significant amount of attention due to the great variety of its applications, including multi-robot systems, transportation, multi-point surveillance and biological systems. The main focus of multi-agent systems is the design of *decentralized* control protocols in order to achieve global tasks, such as *consensus* [1–4], in which all the agents are required to converge to a specific point and *formation* [5–11], in which all the agents aim to form a predefined geometrical shape. At the same time, the agents might need to fulfill certain transient properties, such as *network connectivity* [12–14] and/or *collision avoidance* [15–17]. In parallel, another topic of research is *multi-agent navigation* in both the robotics and the control communities, due to the need for autonomous control of multiple robotic agents in the same workspace. Important applications of multi-agent navigation arise also in the fields of air-traffic management

CONTACT Alexandros Filotheou. Email: alefil@kth.se, Alexandros Nikou. Email: anikou@kth.se and Dimos V. Dimarogonas. Email: dimos@ee.kth.se

and in autonomous driving by guaranteeing collision avoidance with other cars and obstacles. In this work, we study the problem of multi-agent navigation with network connectivity and collision avoidance properties.

The literature on approaching the problem of navigation of multi-agent systems is rich. In [15], ([18]), a decentralized control protocol of multiple non-point agents (point masses) with collision avoidance guarantees is considered. The problem is approached by designing navigation functions which have been initially introduced in [19]. A decentralized potential field approach for navigation of multiple unicycles (aerial vehicles) with collision avoidance has been considered in [20, 21]; Robustness analysis and saturation in control inputs are not addressed. In [22], the collision avoidance problem for multiple agents in intersections has been studied. An optimal control problem is solved, with only time and energy constraints. Authors in [23] proposed decentralized controllers for multi-agent navigation and collision avoidance with arbitrarily shaped obstacles in 2D environments. Furthermore, connectivity maintenance properties are not taken into consideration in all the aforementioned work.

Other approaches in multi-agent navigation propose solutions to decentralized optimization problems. In [24], a decentralized receding horizon protocol for formation control of linear multi-agent systems is proposed. Authors in [25] considered the path-following problems for multiple Unmanned Aerial Vehicles (UAVs) in which a decentralized optimization method is proposed through linearization of the dynamics of the UAVs. A DN MPC along with potential functions for collision avoidance has been studied in [26]. A feedback linearization framework along with Model Predictive Controllers (MPC) for multiple unicycles in leader-follower networks for ensuring collision avoidance and formation is introduced in [27]. Authors in [28–30] propose a decentralized receding horizon approach for discrete time multi-agent cooperative control. However, in the aforementioned works, plant-model mismatch or uncertainties and/or connectivity maintenance are not considered. In [31] ([32]), a centralized (decentralized) linear MPC formulation and integer programming is proposed for dealing with collision avoidance of multiple UAVs.

The contribution of this paper is to provide *decentralized* control protocols which guarantee that a team of rigid-bodies modeled by 2nd order *uncertain* Lagrangian dynamics satisfy: collision avoidance between agents; obstacle avoidance; connectivity preservation; singularity avoidance; that agents remain in the workspace; while the control inputs are saturated. This constitutes a general problem that arises in many multi-agent applications where the agents need to perform a collaborative task, stay close and connected to each other and navigate to desired goal points. To the best of the authors' knowledge, decentralized control protocols that guarantee *all* the aforementioned control specifications for the dynamics in hand have not been proposed in the bibliography. In order to address the aforementioned problem, we propose a Decentralized Nonlinear Model Predictive Control (DN MPC) framework in which each agent solves its own optimal control problem, having availability of information on the current and estimated actions of all agents within its sensing range. The proposed control scheme, under relatively standard Nonlinear Model Predictive Control (NMPC) assumptions, guarantees that all the aforementioned control specifications are satisfied. A conference version of this paper can be found in [33], in which a similar problem is investigated for nonlinear uncertain dynamics with additive disturbance in \mathbb{R}^n , without any rotation representations. However, due to space constraints, the proofs have been omitted in the conference paper.

The remainder of this paper is structured as follows: In Section 2 the notation and preliminaries background are given. Section 3 provides the system dynamics and the

formal problem statement. Section 4 discusses the technical details of the solution and Section 5 is devoted to simulation examples. Finally, conclusions and future work are discussed in Section 6.

2. Notation and Preliminaries

The set of positive integers is denoted by \mathbb{N} . The real n -coordinate space, $n \in \mathbb{N}$, is denoted by \mathbb{R}^n ; $\mathbb{R}_{\geq 0}^n$ and $\mathbb{R}_{>0}^n$ are the sets of real n -vectors with all elements nonnegative and positive, respectively. Given a set S , we denote by $|S|$ its cardinality. The notation $\|\mathbf{x}\|$ is used for the Euclidean norm of a vector $\mathbf{x} \in \mathbb{R}^n$ and $\|\mathbf{A}\| = \max\{\|\mathbf{A}\mathbf{x}\| : \|\mathbf{x}\| = 1\}$ for the induced norm of a matrix $\mathbf{A} \in \mathbb{R}^{m \times n}$. Given a real symmetric matrix \mathbf{A} , $\lambda_{\min}(\mathbf{A})$ and $\lambda_{\max}(\mathbf{A})$ denote the minimum and the maximum absolute value of eigenvalues of \mathbf{A} , respectively. Its minimum and maximum singular values are denoted by $\sigma_{\min}(\mathbf{A})$ and $\sigma_{\max}(\mathbf{A})$ respectively; $\mathbf{I}_n \in \mathbb{R}^{n \times n}$ and $\mathbf{O}_{m \times n} \in \mathbb{R}^{m \times n}$ are the unit matrix and the $m \times n$ matrix with all entries zeros, respectively. The set-valued function $\mathcal{B} : \mathbb{R}^3 \times \mathbb{R}_{>0} \rightrightarrows \mathbb{R}^3$, given by $\mathcal{B}(\mathbf{c}, r) = \{\mathbf{x} \in \mathbb{R}^3 : \|\mathbf{x} - \mathbf{c}\| \leq r\}$, represents the 3D sphere with center $\mathbf{c} \in \mathbb{R}^3$ and radius $r \in \mathbb{R}_{>0}$. Furthermore, we denote by ϕ , θ and ψ the Euler angles of a frame $\{\mathcal{F}\}$ with respect to an inertial frame $\{\mathcal{F}_o\}$. We also use the notation $\mathcal{M} = \mathbb{R}^3 \times \mathcal{T}^3$ where: $\mathcal{T} = (-\pi, \pi) \times (-\frac{\pi}{2}, \frac{\pi}{2}) \times (\pi, \pi)$. For the definitions of Class \mathcal{K} , Class \mathcal{KL} functions, Input-to-State Stability (ISS Stability), ISS Lyapunov Function and positively invariant sets, which will be used thereafter in this manuscript, we refer the reader to [34–36].

Definition 1. (*Minkowski Addition*) Given the sets $\mathcal{S}_1, \mathcal{S}_2 \subseteq \mathbb{R}^n$, their *Minkowski addition* is defined by: $\mathcal{S}_1 \oplus \mathcal{S}_2 = \{s_1 + s_2 \in \mathbb{R}^n : s_1 \in \mathcal{S}_1, s_2 \in \mathcal{S}_2\}$.

Definition 2. (*Pontryagin Difference*) Given the sets $\mathcal{S}_1, \mathcal{S}_2 \subseteq \mathbb{R}^n$, their *Pontryagin difference* is defined by: $\mathcal{S}_1 \ominus \mathcal{S}_2 = \{s_1 \in \mathbb{R}^n : s_1 + s_2 \in \mathcal{S}_1, \forall s_2 \in \mathcal{S}_2\}$.

Property 1. Let the sets $\mathcal{S}_1, \mathcal{S}_2, \mathcal{S}_3 \subseteq \mathbb{R}^n$. Then, it holds that: $(\mathcal{S}_1 \ominus \mathcal{S}_2) \oplus (\mathcal{S}_2 \ominus \mathcal{S}_3) = (\mathcal{S}_1 \oplus \mathcal{S}_2) \ominus (\mathcal{S}_3 \oplus \mathcal{S}_3)$.

Proof. The proof can be found in Appendix A. □

3. Problem Formulation

3.1. System Model

Consider a set \mathcal{V} of N rigid bodies, $\mathcal{V} = \{1, 2, \dots, N\}$, $N \geq 2$, operating in a workspace $W \subseteq \mathbb{R}^3$. A coordinate frame $\{\mathcal{F}_i\}$, $i \in \mathcal{V}$ is attached to the center of mass of each body. The workspace is assumed to be modeled as a bounded sphere $\mathcal{B}(\mathbf{p}_w, r_w)$ expressed in an inertial frame $\{\mathcal{F}_o\}$. We consider that over time t each agent $i \in \mathcal{V}$ occupies the space of a sphere $\mathcal{B}(\mathbf{p}_i(t), r_i)$, where $\mathbf{p}_i : \mathbb{R}_{\geq 0} \rightarrow \mathbb{R}^3$ is the position of the agent's center of mass, and $r_i < r_w$ is the radius of the agent's rigid body. We denote by $\mathbf{q}_i(t) : \mathbb{R}_{\geq 0} \rightarrow \mathcal{T}^3$, the Euler angles representing the agents' orientation with respect to the inertial frame $\{\mathcal{F}_o\}$, with $\mathbf{q}_i \triangleq [\phi_i, \theta_i, \psi_i]^\top$. By defining: $\mathbf{x}_i(t) \triangleq [\mathbf{p}_i(t)^\top, \mathbf{q}_i(t)^\top]^\top$, $\mathbf{x}_i(t) : \mathbb{R}_{\geq 0} \rightarrow \mathcal{M}$, $\mathbf{v}_i(t) \triangleq [\dot{\mathbf{p}}_i(t)^\top, \dot{\boldsymbol{\omega}}_i(t)^\top]^\top$, $\mathbf{v}_i(t) : \mathbb{R}_{\geq 0} \rightarrow \mathbb{R}^6$, we model the motion

of agent i under continuous second order *Lagrangian dynamics* as:

$$\dot{\mathbf{x}}_i(t) = \mathbf{J}(\mathbf{q}_i)\mathbf{v}_i(t), \quad (1a)$$

$$\dot{\mathbf{v}}_i(t) = \mathbf{M}_i^{-1}(\mathbf{x}_i) [-\mathbf{C}_i(\mathbf{x}_i, \dot{\mathbf{x}}_i)\mathbf{v}_i(t) - \mathbf{g}_i(\mathbf{x}_i) + \mathbf{u}_i(t)] + \tilde{\mathbf{w}}_i(\mathbf{x}_i, \mathbf{v}_i, t), \quad (1b)$$

where $\mathbf{J} : \mathcal{T}^3 \rightarrow \mathbb{R}^{6 \times 6}$ is a Jacobian matrix that maps the Euler angle rates to \mathbf{v}_i :

$$\mathbf{J}(\mathbf{q}_i) = \begin{bmatrix} \mathbf{I}_3 & \mathbf{0}_{3 \times 3} \\ \mathbf{0}_{3 \times 3} & \mathbf{J}_q(\mathbf{q}_i) \end{bmatrix}, \quad \mathbf{J}_q(\mathbf{q}_i) = \begin{bmatrix} 1 & \sin \phi_i \tan \theta_i & \cos \phi_i \tan \theta_i \\ 0 & \cos \phi_i & -\sin \phi_i \\ 0 & \frac{\sin \phi_i}{\cos \theta_i} & \frac{\cos \phi_i}{\cos \theta_i} \end{bmatrix}. \quad \text{Moreover, } \mathbf{M}_i :$$

$\mathcal{M} \rightarrow \mathbb{R}^{6 \times 6}$ is the positive definite *inertia matrix*, $\mathbf{C}_i : \mathcal{M} \times \mathbb{R}^6 \rightarrow \mathbb{R}^{6 \times 6}$ is the *Coriolis matrix* and $\mathbf{g}_i : \mathcal{M} \rightarrow \mathbb{R}^6$ is the *gravity vector*. The continuous function $\tilde{\mathbf{w}}_i : \mathcal{M} \times \mathbb{R}^6 \times \mathbb{R}_{\geq 0} \rightarrow \mathbb{R}^6$ is a term representing *disturbances* and *modeling uncertainties*. Finally, $\mathbf{u}_i : \mathbb{R}_{\geq 0} \rightarrow \mathbb{R}^6$ is the control input vector representing the 6D generalized *actuation force* acting on the agent. The aforementioned vectors as well as their derivatives are derived with respect to the inertial frame \mathcal{F}_o . The matrix $\mathbf{J}(\mathbf{q}_i)$ is singular when $\cos \theta_i = 0 \Leftrightarrow \theta_i = \pm \frac{\pi}{2}$. However, the proposed controller guarantees that $\mathbf{J}(\mathbf{q}_i)$ is well-defined for every $i \in \mathcal{V}$.

Let us define the vector $\mathbf{z}_i(t) = [\mathbf{x}_i(t)^\top, \mathbf{v}_i(t)^\top]^\top : \mathbb{R}_{\geq 0} \rightarrow \mathcal{M} \times \mathbb{R}^6$, $i \in \mathcal{V}$. Then, by defining the vector $\dot{\mathbf{z}}_i : \mathbb{R}_{\geq 0} \rightarrow \mathbb{R}^{12}$, the dynamics (1a), (1b) can be written as:

$$\dot{\mathbf{z}}_i(t) = f_i(\mathbf{z}_i(t), \mathbf{u}_i(t)) + \mathbf{w}_i(\mathbf{z}_i(t), t), \quad (2)$$

where $\mathbf{w} = [\mathbf{0}_{1 \times 6}, \tilde{\mathbf{w}}_i^\top]^\top$ and the functions $f_i : \mathcal{M} \times \mathbb{R}^6 \times \mathbb{R}^6 \rightarrow \mathbb{R}^{12}$, $i \in \mathcal{V}$ are given by: $f_i(\mathbf{z}_i(t), \mathbf{u}_i(t)) \triangleq \begin{bmatrix} \mathbf{J}\mathbf{v}_i(t) \\ -\mathbf{M}_i^{-1}[\mathbf{C}_i\mathbf{v}_i(t) + \mathbf{g}_i - \mathbf{u}_i(t)] \end{bmatrix}$. It is assumed that there exist finite constants $\bar{w}_i, \bar{u}_i \in \mathbb{R}_{>0}$, $i \in \mathcal{V}$ such that:

$$\mathcal{W}_i = \{\mathbf{w}_i \in \mathbb{R}^{12} : \|\mathbf{w}_i\| \leq \bar{w}_i\}, \mathcal{U}_i = \{\mathbf{u}_i \in \mathbb{R}^6 : \|\mathbf{u}_i\| \leq \bar{u}_i\}, \quad (3)$$

i.e., the disturbances w_i as well as the control inputs u_i are upper bounded by the terms \bar{w}_i, \bar{u}_i , respectively.

Assumption 1. The nonlinear functions f_i are *locally Lipschitz continuous* in $\mathcal{M} \times \mathbb{R}^6 \times \mathcal{U}_i$ with Lipschitz constants L_{f_i} . Thus, it holds that:

$$\|f_i(\mathbf{z}, \mathbf{u}) - f_i(\mathbf{z}', \mathbf{u})\| \leq L_{f_i} \|\mathbf{z} - \mathbf{z}'\|, \forall \mathbf{z}, \mathbf{z}' \in \mathcal{M} \times \mathbb{R}^6, \mathbf{u} \in \mathcal{U}_i. \quad (4)$$

We consider that in the given workspace there exists a set of $L \in \mathbb{N}$ *static obstacles*, with $\mathcal{L} = \{1, 2, \dots, L\}$, also modeled by the spheres $\mathcal{B}(\mathbf{p}_{o_\ell}, r_{o_\ell})$, with centers at positions $\mathbf{p}_{o_\ell} \in \mathbb{R}^3$ and radii $r_{o_\ell} \in \mathbb{R}_{>0}$, where $\ell \in \mathcal{L}$. Their position and size in the 3D space is assumed to be a priori unknown to each agent. In order for agents to be able to detect the obstacles during their navigation, we assume that each agent $i \in \mathcal{V}$ has a limited spatial obstacle-detection range b_i such that $b_i > r_i$. Thus, each agent senses points which reside on the surface of the obstacles and which are within a radius b_i of its position. Given these points, each agent reconstructs the sphere that corresponds to the obstacle and extracts its position and radius in 3D space.

Assumption 2. (*Measurements Assumption*) Agent $i \in \mathcal{V}$ has: 1) access to measurements $\mathbf{p}_i, \mathbf{q}_i, \dot{\mathbf{p}}_i, \boldsymbol{\omega}_i$, that is, vectors $\mathbf{x}_i, \mathbf{v}_i$ pertaining to itself; 2) A limited sensing

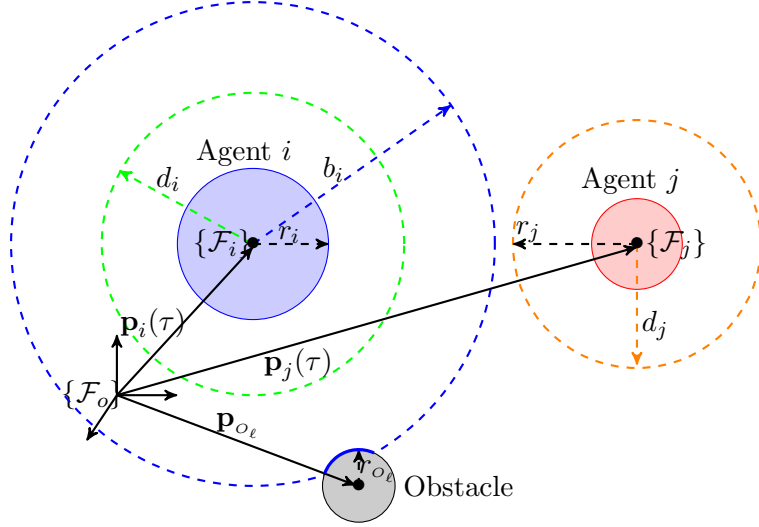


Figure 1.: Illustration of two agents $i, j \in \mathcal{V}$ and a static obstacle $\ell \in \mathcal{L}$ in the workspace at a time instant τ ; $\{\mathcal{O}\}$ is the inertial frame, $\{\mathcal{F}_i\}, \{\mathcal{F}_j\}$ are the frames attached to the agents' center of mass, $\mathbf{p}_i, \mathbf{p}_j, \mathbf{p}_\ell \in \mathbb{R}^3$ are the positions of the centers of mass of agents i, j and obstacle ℓ respectively, expressed in frame $\{\mathcal{F}_o\}$; r_i, r_j, r_ℓ are the radii of the agents i, j and the obstacle ℓ respectively; d_i, d_j with $d_i > d_j$ are the agents' sensing ranges; b_i is the spatial obstacle-detection range of agent i .

range d_i such that: $d_i > \max_{i, j \in \mathcal{V}, i \neq j} \{r_i + r_j\}$.

The latter implies that each agent has sufficiently large sensing radius so as to measure the agent with the biggest volume, due to the fact that the agents' radii are not the same. The consequence of points 1 and 2 of Assumption 2 is that by defining the set of agents j that are within the sensing range of agent i at time t as: $\mathcal{R}_i(t) \triangleq \{j \in \mathcal{V} \setminus \{i\} : \|\mathbf{p}_i(t) - \mathbf{p}_j(t)\| < d_i\}$, agent i knows all signals $\mathbf{p}_j(t), \mathbf{q}_j(t), \dot{\mathbf{p}}_j(t), \boldsymbol{\omega}_j(t), \forall j \in \mathcal{R}_i(t), t \in \mathbb{R}_{\geq 0}$, of all agents $j \in \mathcal{R}_i(t)$ by virtue of being able to calculate them using knowledge of its own $\mathbf{p}_i(t), \mathbf{q}_i(t), \dot{\mathbf{p}}_i(t), \boldsymbol{\omega}_i(t)$. The geometry of two agents i and j as well as an obstacle ℓ in the workspace W is depicted in Figure 1.

Definition 3. (*Collision/Singularity-free Configuration*) The multi-agent system is in a collision/singularity-free configuration at a time instant $\tau \in \mathbb{R}_{\geq 0}$ if all the following hold: 1) For every $i, j \in \mathcal{V}, i \neq j$ it holds that: $\|\mathbf{p}_i(\tau) - \mathbf{p}_j(\tau)\| > r_i + r_j$; 2) For every $i \in \mathcal{V}$ and for every $\ell \in \mathcal{L}$ it holds that: $\|\mathbf{p}_i(\tau) - \mathbf{p}_{o_\ell}\| > r_i + r_{o_\ell}$; 3) For every $i \in \mathcal{V}$ it holds that: $\|\mathbf{p}_i(\tau) - \mathbf{p}_w\| < r_w - r_i$; 4) For every $i \in \mathcal{V}$ it holds that: $-\frac{\pi}{2} < \theta_i(\tau) < \frac{\pi}{2}$.

Definition 4. (*Neighboring set*) Define the *neighboring set* of agent $i \in \mathcal{V}$ as: $\mathcal{N}_i = \{j \in \mathcal{V} \setminus \{i\} : j \in \mathcal{R}_i(0)\}$. We will refer to agents $j \in \mathcal{N}_i$ as the *neighbors* of agent $i \in \mathcal{V}$.

The set \mathcal{N}_i is composed of indices of agents $j \in \mathcal{V}$ which are within the sensing range of agent i at time $t = 0$. Agents $j \in \mathcal{N}_i$ are agents which agent i is instructed to keep within its sensing range at all times $t \in \mathbb{R}_{> 0}$, and therefore maintain connectivity with. While the sets \mathcal{N}_i are introduced for connectivity maintenance specifications and they are fixed, the sets $\mathcal{R}_i(t)$ are used to ensure collision avoidance, and, in general, their composition evolves and varies through time.

Assumption 3. (*Initial Conditions Assumption*) For sake of cooperation needs, we assume that $\mathcal{N}_i \neq \emptyset, \forall i \in \mathcal{V}$ i.e., all agents have at least one neighbor. We also assume that at time $t = 0$ it holds that $\mathbf{v}_i(0) = \mathbf{0}_{6 \times 1}$ and the multi-agent system is in a

collision/singularity-free configuration, as per Definition 3.

3.2. Objectives

Given the aforementioned modeling of the system, the objective of this paper is the *stabilization of the agents* $i \in \mathcal{V}$ starting from a collision/singularity-free configuration as given in Definition 3 to a desired feasible configuration $\mathbf{x}_{i,\text{des}} = [\mathbf{p}_{i,\text{des}}^\top, \mathbf{q}_{i,\text{des}}^\top]^\top \in \mathcal{M}$, while maintaining connectivity between neighboring agents, and avoiding collisions between agents, obstacles, and the workspace boundary.

Definition 5. (*Desired Feasible Configuration*) The desired configuration $\mathbf{x}_{i,\text{des}} = [\mathbf{p}_{i,\text{des}}^\top, \mathbf{q}_{i,\text{des}}^\top]^\top \in \mathcal{M}$ of agents $i \in \mathcal{V}, j \in \mathcal{N}_i$ is *feasible* if the following hold: 1) It is a collision/singularity-free configuration according to Definition 3; 2) It does not result in a violation of the connectivity maintenance between neighboring agents, i.e., $\|\mathbf{p}_{i,\text{des}} - \mathbf{p}_{j,\text{des}}\| < d_i, \forall i \in \mathcal{V}, j \in \mathcal{N}_i$.

Definition 6. (*Feasible Initial Conditions*) Let $\mathbf{x}_{i,\text{des}} = [\mathbf{p}_{i,\text{des}}^\top, \mathbf{q}_{i,\text{des}}^\top]^\top \in \mathcal{M}, i \in \mathcal{V}$ be a desired feasible configuration as defined in Definition 5. Then, the set of all initial conditions $\mathbf{x}_i(0), \mathbf{v}_i(0)$ according to Assumption 3, for which there exist time constants $\bar{t}_i \in \mathbb{R}_{>0} \cup \{\infty\}$ and control inputs $\mathbf{u}_i^* \in \mathcal{U}_i, i \in \mathcal{V}$, which define a solution $\mathbf{x}_i^*(t), t \in [0, \bar{t}_i]$ of the system of differential equations (1a)-(1b), under the presence of disturbance $w_i \in \mathcal{W}_i$, such that: 1) $\mathbf{x}_i^*(\bar{t}_i) = \mathbf{x}_{i,\text{des}}$, 2) $\|\mathbf{p}_i^*(t) - \mathbf{p}_j^*(t)\| > r_i + r_j$ for every $t \in [0, \bar{t}_i], i, j \in \mathcal{V}, i \neq j$, 3) $\|\mathbf{p}_i^*(t) - \mathbf{p}_{o_\ell}\| > r_i + r_{o_\ell}$ for every $t \in [0, \bar{t}_i], i \in \mathcal{V}, \ell \in \mathcal{L}$, 4) $\|\mathbf{p}_i^*(t) - \mathbf{p}_w\| < r_w - r_i$ for every $t \in [0, \bar{t}_i], i \in \mathcal{V}$, 5) $\|\mathbf{p}_i^*(t) - \mathbf{p}_j^*(t)\| < d_i$ for every $t \in [0, \bar{t}_i], i \in \mathcal{V}, j \in \mathcal{N}_i$, are called *feasible initial conditions*.

The feasible initial conditions are, essentially, all the initial conditions $\mathbf{x}_i(0), \mathbf{v}_i(0), i \in \mathcal{V}$ from which there exist controllers $u_i \in \mathcal{U}_i$ that can navigate the agents to the given desired states $\mathbf{x}_{i,\text{des}}$, under the presence of disturbances $w_i \in \mathcal{W}_i$, while i) the initial neighbors remain connected, ii) the agents do not collide with each other, iii) the agents stay in the workspace and iv) the agents do not collide with the obstacles of the environment. Initial conditions for which one or more agents can not be driven to the desired state $\mathbf{x}_{i,\text{des}}$ by a controller $u_i \in \mathcal{U}_i$, i.e., initial conditions that violate one or more of the conditions of Definition 6, are considered *infeasible initial conditions*. Motivated by this observation, the goal of this paper is to provide a systematic method of designing decentralized feedback controllers that navigate the agents to the desired states $\mathbf{x}_{i,\text{des}}$ from all *feasible initial conditions*, as defined in Definition 6.

3.3. Problem Statement

Formally, the control problem, under the aforementioned constraints, is formulated as follows:

Problem 1. Consider N agents governed by dynamics (2), modeled by the spheres $\mathcal{B}(\mathbf{p}_i, r_i), i \in \mathcal{V}$, and operating in a spherical workspace W which is modeled by the sphere $\mathcal{B}(\mathbf{p}_w, r_w)$. In the workspace there are L spherical obstacles $\mathcal{B}(\mathbf{p}_{o_\ell}, r_{o_\ell}), \ell \in \mathcal{L}$. The agents have communication capabilities according to Assumption 2, under the initial conditions $\mathbf{x}_i(0), \mathbf{v}_i(0)$ imposed by Assumption 3 and they are affected by disturbances $w_i \in \mathcal{W}_i$. Then, given a desired feasible configuration $\mathbf{x}_{i,\text{des}}$ according to

Definition 5, for all feasible initial conditions, as defined in Definition 6, the problem lies in designing decentralized feedback control laws $\mathbf{u}_i \in \mathcal{U}_i$, such that for every $i \in \mathcal{V}$ and for all times $t \in \mathbb{R}_{\geq 0}$, all the following specifications are satisfied: 1) Position and orientation stabilization is achieved: $\lim_{t \rightarrow \infty} \|\mathbf{x}_i(t) - \mathbf{x}_{i,\text{des}}\| \rightarrow 0$; 2) Inter-agent collision is avoided: $\|\mathbf{p}_i(t) - \mathbf{p}_j(t)\| > r_i + r_j, \forall j \in \mathcal{V}, j \neq i$; 3) Connectivity between neighboring agents is preserved: $\|\mathbf{p}_i(t) - \mathbf{p}_j(t)\| < d_i, \forall j \in \mathcal{N}_i$; 4) Agent-with-obstacle collision is avoided: $\|\mathbf{p}_i(t) - \mathbf{p}_{o_\ell}(t)\| > r_i + r_{o_\ell}, \forall \ell \in \mathcal{L}$; 5) Agent-with-workspace-boundary collision is avoided: $\|\mathbf{p}_i(t) - \mathbf{p}_w\| < r_w - r_i$; 6) All matrices $\mathbf{J}(\mathbf{q}_i)$ are well defined: $-\frac{\pi}{2} < \theta_i(t) < \frac{\pi}{2}$;

4. Proposed Solution

In this section, a systematic solution to Problem 1 is introduced. Our overall approach builds on designing a decentralized control law $\mathbf{u}_i \in \mathcal{U}_i$, $i \in \mathcal{V}$ for each agent. In particular, since we aim to minimize the norms $\|\mathbf{x}_i(t) - \mathbf{x}_{i,\text{des}}\|$ as $t \rightarrow \infty$, subject to the state constraints imposed by Problem 1, it is reasonable to seek a solution which is the outcome of an optimization problem. In Section 4.1 we derive the error dynamics and in Section 4.2 we discuss the proposed control scheme as well as the stability analysis.

4.1. Error Dynamics

Let us define the stack vector of the desired states and velocities by: $\mathbf{z}_{i,\text{des}} = \begin{bmatrix} \mathbf{x}_{i,\text{des}}^\top, \mathbf{v}_{i,\text{des}}^\top \end{bmatrix}^\top \in \mathcal{M} \times \mathbb{R}^6$. The state $\mathbf{x}_{i,\text{des}} \in \mathcal{M}$ is the desired feasible state that agent i needs to reach, as is given in Problem 1. For the desired velocities $\mathbf{v}_{i,\text{des}} \in \mathbb{R}^6$ we can set, without loss of generality, that $\mathbf{v}_{i,\text{des}} = \mathbf{0}_{6 \times 1}$, i.e., the agents need to stop when they achieve the desired state. We define the error vector $\mathbf{e}_i : \mathbb{R}_{\geq 0} \rightarrow \mathcal{M} \times \mathbb{R}^6$ by:

$$\mathbf{e}_i(t) = \begin{bmatrix} \mathbf{x}_i(t) \\ \mathbf{v}_i(t) \end{bmatrix} - \begin{bmatrix} \mathbf{x}_{i,\text{des}} \\ \mathbf{v}_{i,\text{des}} \end{bmatrix} = \mathbf{z}_i(t) - \mathbf{z}_{i,\text{des}}. \quad (5)$$

If we provide a control scheme that guarantees that $\lim_{t \rightarrow \infty} \|\mathbf{z}_i(t) - \mathbf{z}_{i,\text{des}}\| \rightarrow 0$ then it is also guaranteed that $\lim_{t \rightarrow \infty} \|\mathbf{x}_i(t) - \mathbf{x}_{i,\text{des}}\| \rightarrow 0$, which is the first goal of Problem 1. By defining the vector $\dot{\mathbf{e}}_i : \mathbb{R}_{\geq 0} \rightarrow \mathbb{R}^{12}$, the *error dynamics* are given by:

$$\dot{\mathbf{e}}_i(t) = h_i(\mathbf{e}_i(t), \mathbf{u}_i(t)), \quad (6)$$

where the functions $h_i : \mathcal{M} \times \mathbb{R}^6 \times \mathbb{R}^6 \rightarrow \mathbb{R}^{12}$, $g_i : \mathcal{M} \times \mathbb{R}^6 \times \mathbb{R}^6 \rightarrow \mathbb{R}^{12}$ are defined by:

$$h_i(\mathbf{e}_i(t), \mathbf{u}_i(t)) \triangleq g_i(\mathbf{e}_i(t), \mathbf{u}_i(t)) + \mathbf{w}_i(\mathbf{e}_i(t) + \mathbf{z}_{i,\text{des}}, t), \quad (7a)$$

$$g_i(\mathbf{e}_i(t), \mathbf{u}_i(t)) \triangleq f_i(\mathbf{e}_i(t) + \mathbf{z}_{i,\text{des}}, \mathbf{u}_i(t)), \quad (7b)$$

respectively, where f_i is defined in (2). We define the set $\mathcal{Z}_i \subseteq \mathcal{M} \times \mathbb{R}^6$, $i \in \mathcal{V}$ as the set that captures all the *state* constraints on the system (1), posed by Problem 1.

Therefore \mathcal{Z}_i is given by:

$$\begin{aligned} \mathcal{Z}_i \triangleq & \left\{ \mathbf{z}_i(t) \in \mathcal{M} \times \mathbb{R}^6 : \|\mathbf{p}_i(t) - \mathbf{p}_j(t)\| \geq r_i + r_j + \varepsilon, \forall j \in \mathcal{R}_i(t), \right. \\ & \|\mathbf{p}_i(t) - \mathbf{p}_j(t)\| \leq d_i - \varepsilon, \forall j \in \mathcal{N}_i, \|\mathbf{p}_i(t) - \mathbf{p}_{o_\ell}\| \geq r_i + r_{o_\ell} + \varepsilon, \forall \ell \in \mathcal{L}, \\ & \left. \|\mathbf{p}_i(t) - \mathbf{p}_w\| \leq r_w - r_i - \varepsilon, -\frac{\pi}{2} + \varepsilon \leq \theta_i(t) \leq \frac{\pi}{2} - \varepsilon \right\}, i \in \mathcal{V}, \end{aligned}$$

where $\varepsilon \in \mathbb{R}_{>0}$ is an arbitrary small constant. In order to translate the constraints that are dictated for the state z_i into constraints regarding the error state e_i of (5), we define the set $\mathcal{E}_i = \{\mathbf{e}_i \in \mathcal{M} \times \mathbb{R}^6 : \mathbf{e}_i \in \mathcal{Z}_i \oplus (-\mathbf{z}_{i,\text{des}})\}$, $\forall i \in \mathcal{V}$. Then, the following rudimentary equivalence holds for all $i \in \mathcal{V}$: $\mathbf{z}_i \in \mathcal{Z}_i \Leftrightarrow \mathbf{e}_i \in \mathcal{E}_i$.

Property 2. The nonlinear functions g_i , $i \in \mathcal{V}$ as defined in (7b), are *locally Lipschitz continuous* in $\mathcal{E}_i \times \mathcal{U}_i$, with Lipschitz constants $L_{g_i} = L_{f_i}$, where L_{f_i} as in (4). Thus,

$$\|g_i(\mathbf{e}, \mathbf{u}) - g_i(\mathbf{e}', \mathbf{u})\| \leq L_{g_i} \|\mathbf{e} - \mathbf{e}'\|, \forall \mathbf{e}, \mathbf{e}' \in \mathcal{E}_i, \mathbf{u} \in \mathcal{U}_i. \quad (8)$$

Proof. The proof can be found in Appendix B. □

The goal is to solve Problem 1, i.e, to design decentralized control laws $\mathbf{u}_i \in \mathcal{U}_i$, $\forall i \in \mathcal{V}$ such that the error signal \mathbf{e}_i , with dynamics as in (6), constrained by $\mathbf{e}_i \in \mathcal{E}_i$, satisfies $\lim_{t \rightarrow \infty} \|\mathbf{e}_i(t)\| \rightarrow 0$, while all system signals remain bounded in their respective regions as well.

4.2. Decentralized Control Design

Due to the fact that we have to deal with the minimization of norms $\|\mathbf{e}_i(t)\|$, as $t \rightarrow \infty$, subject to constraints $e_i \in \mathcal{E}_i$, we invoke here a class of decentralized Nonlinear Model Predictive controllers (NMPC). NMPC frameworks have been studied in [37–45] and they have been proven to be a powerful tool for dealing with state and input constraints.

Consider a sequence of sampling times $\{t_k\}_{k \in \mathbb{N}}$, with a constant sampling time h , $0 < h < T_p$, where T_p is the finite time predicted horizon, such that $t_{k+1} = t_k + h$, $\forall k \in \mathbb{N}$. Hereafter we will denote by i the agent and by index k the sampling instant. In sampled data NMPC, a Finite-Horizon Open-loop Optimal Control Problem (FHOCP) is solved at discrete sampling time instants t_k based on the current state error measurement $\mathbf{e}_i(t_k)$. The solution is an optimal control signal $\bar{\mathbf{u}}_i^*(s)$, computed over $s \in [t_k, t_k + T_p]$. The open-loop input signal applied in between the sampling instants is given by the solution of the following FHOCP:

$$\begin{aligned} & \min_{\bar{\mathbf{u}}_i(\cdot)} J_i(\mathbf{e}_i(t_k), \bar{\mathbf{u}}_i(\cdot)) \\ & = \min_{\bar{\mathbf{u}}_i(\cdot)} \left\{ V_i(\bar{\mathbf{e}}_i(t_k + T_p)) + \int_{t_k}^{t_k + T_p} [F_i(\bar{\mathbf{e}}_i(s), \bar{\mathbf{u}}_i(s))] ds \right\} \end{aligned} \quad (9a)$$

subject to:

$$\dot{\bar{\mathbf{e}}}(s) = g_i(\bar{\mathbf{e}}_i(s), \bar{\mathbf{u}}_i(s)), \bar{\mathbf{e}}_i(t_k) = \mathbf{e}_i(t_k), \quad (9b)$$

$$\bar{\mathbf{e}}_i(s) \in \mathcal{E}_{i,s-t_k}, \bar{\mathbf{u}}_i(s) \in \mathcal{U}_i, s \in [t_k, t_k + T_p], \quad (9c)$$

$$\bar{\mathbf{e}}(t_k + T_p) \in \Omega_i. \quad (9d)$$

At a generic time t_k then, agent $i \in \mathcal{V}$ solves the aforementioned FHOCP. The notation $\bar{\cdot}$ is used to distinguish predicted states which are internal to the controller, corresponding to the nominal system (9b) (i.e., the system (6) by substituting $\mathbf{w} = \mathbf{0}_{12 \times 1}$). This means that $\bar{\mathbf{e}}_i(\cdot)$ is the solution to (9b) driven by the control input $\bar{\mathbf{u}}_i(\cdot) : [t_k, t_k + T_p] \rightarrow \mathcal{U}_i$ with initial condition $\mathbf{e}_i(t_k)$. Note that the predicted states are not the same with the actual closed-loop values due to the fact that the system is under the presence of disturbances $w_i \in \mathcal{W}_i$, where \mathcal{W}_i is defined in (3). The functions $F_i : \mathcal{E}_i \times \mathcal{U}_i \rightarrow \mathbb{R}_{\geq 0}$, $V_i : \mathcal{E}_i \rightarrow \mathbb{R}_{\geq 0}$ stand for the *running costs* and the *terminal penalty costs*, respectively, and they are defined by:

$$F_i(\bar{\mathbf{e}}_i, \bar{\mathbf{u}}_i) \triangleq \bar{\mathbf{e}}_i^\top \mathbf{Q}_i \bar{\mathbf{e}}_i + \bar{\mathbf{u}}_i^\top \mathbf{R}_i \bar{\mathbf{u}}_i, \quad (10a)$$

$$V_i(\bar{\mathbf{e}}_i) \triangleq \bar{\mathbf{e}}_i^\top \mathbf{P}_i \bar{\mathbf{e}}_i. \quad (10b)$$

$\mathbf{R}_i \in \mathbb{R}^{6 \times 6}$ and $\mathbf{Q}_i, \mathbf{P}_i \in \mathbb{R}^{12 \times 12}$ are symmetric and positive definite controller gain matrices to be appropriately tuned. The sets $\mathcal{E}_{i,s-t_k}$, Ω_i will be explained later. For the running cost functions F_i , $i \in \mathcal{V}$ the following hold:

Lemma 1. *Let the running costs F_i be defined by (10a). Then, for all $\boldsymbol{\eta}_i \in \mathcal{E}_i \times \mathcal{U}_i$, there exist functions $\alpha_1, \alpha_2 \in \mathcal{K}_\infty$ such that: $\alpha_1(\|\boldsymbol{\eta}_i\|) \leq F_i(\mathbf{e}_i, \mathbf{u}_i) \leq \alpha_2(\|\boldsymbol{\eta}_i\|)$, $i \in \mathcal{V}$, where $\boldsymbol{\eta}_i \triangleq [\mathbf{e}_i^\top, \mathbf{u}_i^\top]^\top$.*

Proof. The proof can be found in Appendix C. □

Lemma 2. *The running costs F_i are locally Lipschitz continuous in $\mathcal{E}_i \times \mathcal{U}_i$. Thus, it holds that: $|F_i(\mathbf{e}_i, \mathbf{u}_i) - F_i(\mathbf{e}'_i, \mathbf{u}_i)| \leq L_{F_i} \|\mathbf{e}_i - \mathbf{e}'_i\|$, $\forall \mathbf{e}_i, \mathbf{e}'_i \in \mathcal{E}_i, \mathbf{u} \in \mathcal{U}_i$, where: $L_{F_i} \triangleq 2\sigma_{\max}(\mathbf{Q}_i) \sup_{\mathbf{e}_i \in \mathcal{E}_i} \|\mathbf{e}_i\|$.*

Proof. The proof can be found in Appendix D. □

The applied input signal is a portion of the optimal solution to an optimization problem where information on the states of the neighboring agents of agent i is taken into account only in the constraints considered in the optimization problem. These constraints pertain to the set of its neighbors \mathcal{N}_i and, in total, to the set of all agents within its sensing range \mathcal{R}_i . Regarding these, we make the following assumption:

Assumption 4. (*Access to Predicted Information from each agent*) When at time t_k agent i solves a FHOCP, it has access to the following measurements, across the entire horizon $s \in (t_k, t_k + T_p]$:

- (1) Measurements of the states:
 - $\mathbf{z}_j(t_k)$ of all agents $j \in \mathcal{R}_i(t_k)$ within its sensing range at time t_k ;
 - $\mathbf{z}_{j'}(t_k)$ of all of its neighboring agents $j' \in \mathcal{N}_i$ at time t_k ;
- (2) The *predicted states*:
 - $\bar{\mathbf{z}}_j(s)$ of all agents $j \in \mathcal{R}_i(t_k)$ within its sensing range;
 - $\bar{\mathbf{z}}_{j'}(s)$ of all of its neighboring agents $j' \in \mathcal{N}_i$;

Remark 1. The justification for this assumption is as follows. By considering that $\mathcal{N}_i \subseteq \mathcal{R}_i(t)$, $\forall t \in \mathbb{R}_{\geq 0}$, that the state vectors \mathbf{z}_j are comprised of 12 real numbers encoded by 4 bytes, and that the sampling occurs with a frequency f for all agents, the overall downstream bandwidth required by each agent is: $BW_d = 12 \times 32$ [bits] $\times |\mathcal{R}_i| \times \frac{T_p}{h} \times f$ [sec^{-1}]. Given a conservative sampling time $f = 100$ Hz and a horizon of

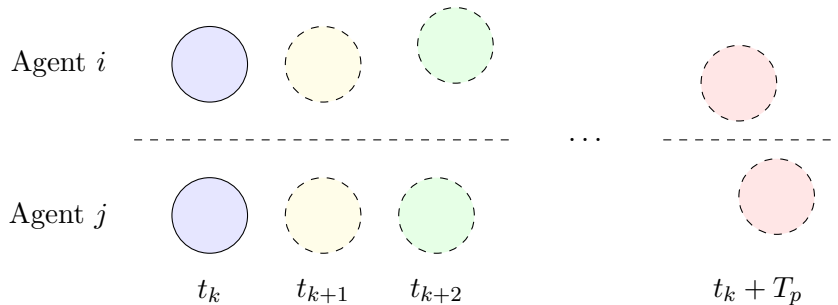


Figure 2.: The inter-agent constraint regime for two agents, i, j . Fully outlined circles denote measured configurations, while partly outlined circles denote predicted configurations. During the solution to the individual optimization problems, the predicted configuration of each agent at each time step is constrained by the predicted configuration of the other agent at the same time step (hence the homologously identical colors at each discrete time step).

$\frac{T_p}{h} = 100$ time steps, the wireless protocol IEEE 802.11n-2009 (a standard for present-day devices) can accommodate up to $|\mathcal{R}_i| = \frac{600 \text{ [Mbit} \cdot \text{sec}^{-1}]}{12 \times 32 \text{ [bit]} \times 10^4 \text{ [sec}^{-1}]} \approx 16 \cdot 10^2$ agents, within the range of one agent. We deem this number to be large enough for practical applications for the approach of assuming access to the predicted states of agents within the range of one agent to be reasonable.

In other words, each time an agent solves its own individual optimization problem, it knows the (open-loop) state predictions that have been generated by the solution of the optimization problem of all agents within its sensing range at that time, for the next T_p time units. These pieces of information are required, as each agent's trajectory is constrained not by constant values, but by the trajectories of its associated agents through time: at each solution time t_k and within the next T_p time units, an agent's predicted configuration at time $s \in [t_k, t_k + T_p]$ needs to be constrained by the predicted configuration of its neighboring and perceivable agents (agents within its sensing range) at the same time instant s , so that collisions are avoided, and connectivity between neighboring agents is maintained. We assume that the above pieces of information are *always available, accurate* and can be exchanged *without delay*. Figure 2 depicts the designed inter-agent (and intra-horizon) constraint regime.

Remark 2. The designed procedure flow can be either concurrent or sequential, meaning that agents can solve their individual FHOCPs and apply the control inputs either simultaneously, or one after the other. The conceptual design itself is procedure-flow agnostic, and hence it can incorporate both without loss of feasibility or successful stabilization. The approach that we have adopted here is the sequential one: each agent solves its own FHOCP and applies the corresponding admissible control input in a round robin way, considering the current and planned (open-loop state predictions) configurations of all agents within its sensing range. This choice is made on account of three reasons: (a) Safety: if a parallel approach is adopted, at the limit, that is in the event that the communication (maximum distance) range is comparable to the size of the agents (consider for instance the case where two UAVs need to collaboratively transport a similar-sized object) it is more likely for collisions to occur. This is because, within a parallel approach, agents would need to rely more on the open-loop predictions of their neighboring agents, which, in the case of disturbances, would make the violation of constraints more likely to occur. (b) Conversely, the sequential

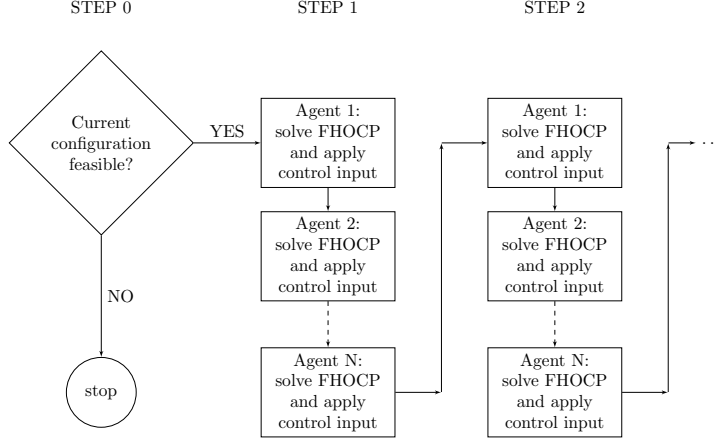


Figure 3.: The procedure is approached sequentially. Notice that the figure implies that recursive feasibility is established if the initial configuration is itself feasible.

approach allows each agent, in turn, to have access to the direct measurements of all other agents' position and overall configuration, as well as their predicted trajectories, *before* solving its own optimization problem, thereby allowing agents to plan their trajectories and execute their motions using additional and concrete information on top of the (in principle approximate) open-loop predictions, and therefore without danger of violating their constraints. (c) Synchronization problems between agents are avoided within a sequential approach, since, from the moment when agent $i \in \mathcal{V}$ starts to solve its optimization problem to the moment that it concludes executing its motion, all agents $j \in \mathcal{V}, j \neq i$ are assumed stationary, while the configuration of those within its sensing range is known to i . Figure 3 and Figure 4 depict the sequential procedural and informational regimes.

The solution to FHOCP (9a) - (9d) at time t_k provides an optimal control input, denoted by $\bar{\mathbf{u}}_i^*(s; \mathbf{e}_i(t_k))$, $s \in [t_k, t_k + T_p]$. This control input is then applied to the system until the next sampling instant t_{k+1} :

$$\mathbf{u}_i(s; \mathbf{e}_i(t_k)) = \bar{\mathbf{u}}_i^*(s; \mathbf{e}_i(t_k)), \quad s \in [t_k, t_{k+1}). \quad (11)$$

At time t_{k+1} a new finite horizon optimal control problem is solved in the same manner, leading to a receding horizon approach.

The control input $\mathbf{u}_i(\cdot)$ is of feedback form, since it is recalculated at each sampling instant based on the then-current state. The solution of (6) at time s , $s \in [t_k, t_k + T_p]$, starting at time t_k , from an initial condition $\mathbf{e}_i(t_k) = \bar{\mathbf{e}}_i(t_k)$, by application of the control input $\mathbf{u}_i : [t_k, s] \rightarrow \mathcal{U}_i$ is denoted by: $\mathbf{e}_i(s; \mathbf{u}_i(\cdot), \mathbf{e}_i(t_k))$, $s \in [t_k, t_k + T_p]$.

The *predicted* state of the system (9b) at time s , $s \in [t_k, t_k + T_p]$ based on the measurement of the state at time t_k , $\mathbf{e}_i(t_k)$, by application of the control input $\mathbf{u}_i(s; \mathbf{e}_i(t_k))$, for the time period $s \in [t_k, t_k + T_p]$ is denoted by: $\bar{\mathbf{e}}_i(s; \mathbf{u}_i(\cdot), \mathbf{e}_i(t_k))$, $s \in [t_k, t_k + T_p]$.

Due to the fact that the system is in presence of disturbances $w_i \in \mathcal{W}_i$, as \mathcal{W}_i defined in (3), it holds in general that: $\bar{\mathbf{e}}_i(\cdot) \neq \mathbf{e}_i(\cdot)$.

Property 3. By integrating (6), (9b) at the time interval $s \geq \tau$, the actual $\mathbf{e}_i(\cdot)$ and

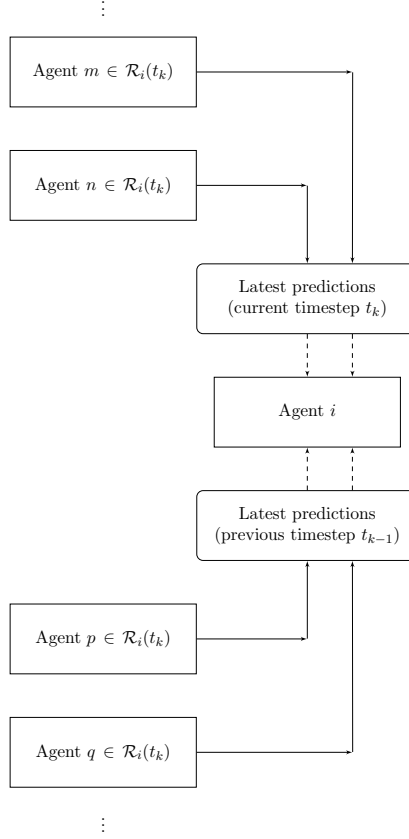


Figure 4.: The flow of information to agent i regarding his perception of agents within its sensing range \mathcal{R}_i at arbitrary FHOCP solution time t_k . Agents $m, n \in \mathcal{R}_i(t_k)$ have solved their FHOCP; agent i is next; agents $p, q \in \mathcal{R}_i(t_k)$ have not solved their FHOCP yet.

the predicted states $\bar{\mathbf{e}}_i(\cdot)$ are respectively given by:

$$\mathbf{e}_i(s; \mathbf{u}_i(\cdot), \mathbf{e}_i(\tau)) = \mathbf{e}_i(\tau) + \int_{\tau}^s h_i(\mathbf{e}_i(s'; \mathbf{e}_i(\tau)), \mathbf{u}_i(s)) ds', \quad (12a)$$

$$\bar{\mathbf{e}}_i(s; \mathbf{u}_i(\cdot), \mathbf{e}_i(\tau)) = \mathbf{e}_i(\tau) + \int_{\tau}^s g_i(\bar{\mathbf{e}}_i(s'; \mathbf{e}_i(\tau)), \mathbf{u}_i(s')) ds'. \quad (12b)$$

The satisfaction of the constraints \mathcal{E}_i on the state along the prediction horizon depends on the future realization of the uncertainties. Through the assumption of additive uncertainty and Lipschitz continuity of the nominal model, it is possible to compute a bound on the future effect of the uncertainty on the system. Then, by considering this effect on the state constraint on the nominal prediction, it is possible to guarantee that the evolution of the real state of the system will be admissible for all times. In view of the latter, the state constraint set \mathcal{E}_i of the standard NMPC formulation, is being replaced by a restricted constraint set $\mathcal{E}_{s-t_k} \subseteq \mathcal{E}_i$ in (9c). This state constraints' tightening for the nominal system (9b) with additive disturbance $\mathbf{w}_i \in \mathcal{W}_i$ is a key ingredient of the proposed controller and guarantees that the evolution of the real system will be admissible for all times. If the state constraint set was left unchanged during the solution of the optimization problem, the applied input

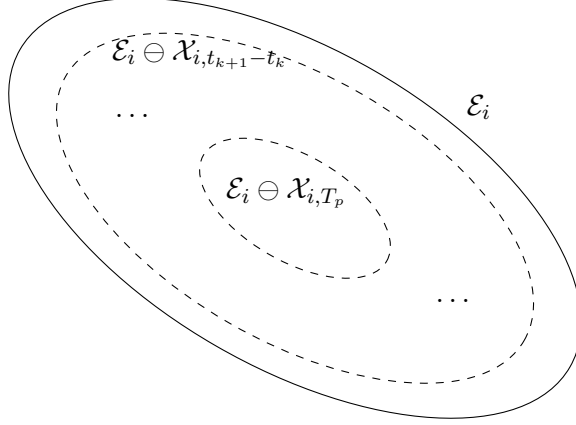


Figure 5.: The nominal constraint set \mathcal{E}_i in bold, and the consecutive restricted constraint sets $\mathcal{E}_i \ominus \mathcal{X}_{i, s-t_k}$, $s \in [t_k, t_k + T_p]$, dashed. The predicted state is constrained by a different and more tight set at each different time instant, since the more times goes by the more uncertain the true state becomes, and hence, the more the model state needs to be restricted if the true state is to be constrained within \mathcal{E}_i at all times.

to the plant, coupled with the uncertainty affecting the states of the plant could force the states of the plant to escape their intended bounds. The aforementioned tightening set strategy is inspired by the works [46–48].

Lemma 3. *The difference between the actual measurement $\mathbf{e}_i(t_k + s; \mathbf{u}_i(\cdot), \mathbf{e}_i(t_k))$ at time $t_k + s$, $s \in (0, T_p]$, and the predicted state $\bar{\mathbf{e}}_i(t_k + s; \mathbf{u}_i(\cdot), \mathbf{e}_i(t_k))$ at the same time, under a control input $\mathbf{u}_i(\cdot) \in \mathcal{U}_i$, starting at the same initial state $\mathbf{e}_i(t_k)$ is upper bounded by: $\|\mathbf{e}_i(t_k + s; \mathbf{u}_i(\cdot), \mathbf{e}_i(t_k)) - \bar{\mathbf{e}}_i(t_k + s; \mathbf{u}_i(\cdot), \mathbf{e}_i(t_k))\| \leq \frac{\bar{w}_i}{L_{g_i}}(e^{L_{g_i}s} - 1)$, $s \in (0, T_p]$, where \bar{w}_i is the upper bound of the disturbance as defined in (3), and L_{g_i} is defined in (8).*

Proof. The proof can be found in Appendix E. □

By taking into consideration the aforementioned Lemma, the restricted constraints set are then defined by: $\mathcal{E}_{i, s-t_k} \triangleq \mathcal{E}_i \ominus \mathcal{X}_{i, s-t_k}$, where:

$$\mathcal{X}_{i, s-t_k} = \left\{ \mathbf{e}_i \in \mathcal{M} \times \mathbb{R}^6 : \|\mathbf{e}_i(s)\| \leq \frac{\bar{w}_i}{L_{g_i}}(e^{L_{g_i}(s-t_k)} - 1), \forall s \in [t_k, t_k + T_p] \right\}. \quad (13)$$

If the state constraint set considered in the solution of the FHOC is given by: $\mathcal{E}_{i, s-t_k}$, then the state of the real system \mathbf{e}_i is guaranteed to fulfill the original state constraint sets \mathcal{E}_i . We formalize this statement in Property 4.

Property 4. For every $s \in [t_k, t_k + T_p]$, it holds that if: $\bar{\mathbf{e}}_i(s; \mathbf{u}_i(\cdot), \mathbf{e}_i(t_k)) \in \mathcal{E}_i \ominus \mathcal{X}_{i, s-t_k}$, where $\mathcal{X}_{i, s-t_k}$ is given by (13), then the real state \mathbf{e}_i satisfies the constraints \mathcal{E}_i , i.e., $\mathbf{e}_i(s) \in \mathcal{E}_i$.

Proof. The proof can be found in Appendix F. □

Assumption 5. The terminal set Ω_i is a subset of an admissible and positively invariant set Ψ_i , with $\Omega_i \subseteq \Psi_i$, where Ψ_i is defined by: $\Psi_i \triangleq \{\bar{\mathbf{e}}_i \in \Phi_i : V_i(\bar{\mathbf{e}}_i) \leq \varepsilon_{\Psi_i}\}$, $\varepsilon_{\Psi_i} > 0$.

Assumption 6. The set Ψ_i is interior to the set Φ_i , $\Psi_i \subseteq \Phi_i$, which is the set of states within \mathcal{E}_{i,T_p-h} for which there exists an admissible control input (see Definition 7) which is of linear feedback form with respect to the state $\kappa_i(\mathbf{e}_i) : [0, h] \rightarrow \mathcal{U}_i$: $\bar{\Phi}_i \triangleq \{\bar{\mathbf{e}}_i \in \mathcal{E}_{i,T_p-h} : \kappa_i(\bar{\mathbf{e}}_i) \in \mathcal{U}_i\}$, such that for all $\mathbf{e}_i \in \Psi_i$ and for all $s \in [0, h]$ it holds that:

$$\frac{\partial V_i}{\partial \mathbf{e}_i} g_i(\mathbf{e}_i(s), \kappa_i(\mathbf{e}_i(s))) + F_i(\mathbf{e}_i(s), \kappa_i(\mathbf{e}_i(s))) \leq 0. \quad (14)$$

Remark 3. The existence of the robust linear state-feedback control law κ_i is ensured if: 1) the linearization of system (6) is stabilizable; 2) the function h_i is twice differentiable, *locally Lipschitz continuous* in $\mathcal{E}_i \times \mathcal{U}_i$ with $f(\mathbf{0}, \mathbf{0}) = \mathbf{0}$, and 3) \mathcal{U}_i is a compact subset of \mathbb{R}^6 containing the origin in its interior [49, 50].

Assumption 7. The admissible and positively invariant set Ψ_i is such that $\forall \mathbf{e}_i(t) \in \Psi_i \Rightarrow \bar{\mathbf{e}}_i(t+s; \kappa_i(\mathbf{e}_i(t)), \mathbf{e}_i(t)) \in \Omega_i \subseteq \Psi_i$, for some $s \in [0, h]$.

The terminal sets Ω_i are chosen to be closed, including the origin, as: $\Omega_i \triangleq \{\bar{\mathbf{e}}_i \in \mathcal{E}_i : V_i(\bar{\mathbf{e}}_i) \leq \varepsilon_{\Omega_i}\}$, where $\varepsilon_{\Omega_i} \in (0, \varepsilon_{\Psi_i})$.

Remark 4. It should be noted that the larger the length of the time-horizon T_p the more probable (in general) it becomes that the sets $\mathcal{E}_{i,s}$ may become empty beyond some $s \in [t_k, t_k + T_p]$. The length of the time-horizon should hence be designed so that the above violation does not occur.

For the terminal cost penalty functions V_i , $i \in \mathcal{V}$ the following hold:

Lemma 4. *Let the functions V_i be defined by (10b). Then, for every $\mathbf{e}_i \in \Psi_i$ there exist functions $\alpha_1, \alpha_2 \in \mathcal{K}_\infty$ such that: $\alpha_1(\|\mathbf{e}_i\|) \leq V_i(\mathbf{e}_i) \leq \alpha_2(\|\mathbf{e}_i\|)$, $\forall i \in \mathcal{V}$.*

Proof. The proof can be found in Appendix G. □

Lemma 5. *The terminal penalty functions V_i are locally Lipschitz continuous in Ψ_i . Thus it holds that: $|V_i(\mathbf{e}_i) - V_i(\mathbf{e}'_i)| \leq L_{V_i} \|\mathbf{e}_i - \mathbf{e}'_i\|$, $\forall \mathbf{e}_i, \mathbf{e}'_i \in \Psi_i$, where: $L_{V_i} = 2\sigma_{\max}(\mathbf{P}_i) \sup_{\mathbf{e}_i \in \Psi_i} \|\mathbf{e}_i\|$.*

Proof. The proof is similar to the proof of Lemma 2 and is omitted. □

We can now give the definition of an *admissible input* for the FHOCP (9a)-(9d).

Definition 7. (Admissible input for FHOCP (9a)-(9d)) A control input $\mathbf{u}_i : [t_k, t_k + T_p] \rightarrow \mathbb{R}^6$ for a state $\mathbf{e}_i(t_k)$ is called *admissible* for the problem (9a)-(9d) if the following hold: 1) $\mathbf{u}_i(\cdot)$ is piecewise continuous; 2) $\mathbf{u}_i(s) \in \mathcal{U}_i$, $\forall s \in [t_k, t_k + T_p]$; 3) $\bar{\mathbf{e}}_i(t_k + s; \mathbf{u}_i(\cdot), \mathbf{e}_i(t_k)) \in \mathcal{E}_i \ominus \mathcal{X}_{i,s}$, $\forall s \in [0, T_p]$; 4) $\bar{\mathbf{e}}_i(t_k + T_p; \mathbf{u}_i(\cdot), \mathbf{e}_i(t_k)) \in \Omega_i$;

In other words, \mathbf{u}_i is admissible if it conforms to the constraints on the input and its application yields states that conform to the prescribed state constraints of FHOCP (9a)-(9d) along the entire horizon $[t_k, t_k + T_p]$, and the terminal predicted state conforms to the terminal constraint.

Under these considerations, we can now state the theorem that relates to the guaranteeing of the stability of the compound system of agents $i \in \mathcal{V}$, when each of them is assigned a desired position and orientation:

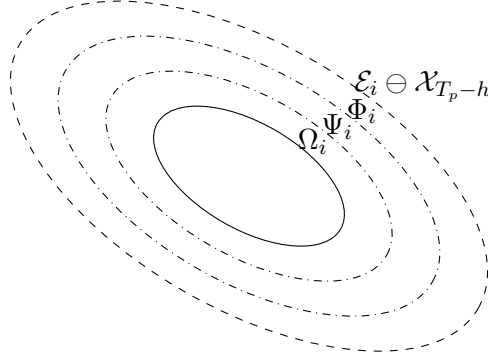


Figure 6.: The hierarchy of sets $\Omega_i \subseteq \Psi_i \subseteq \Phi_i \subseteq \mathcal{E}_i \ominus \mathcal{X}_{T_p-h}$, in bold, dash-dotted, dashed, and dashed, respectively. For every state in Φ_i there is a linear state feedback control $\kappa_i(\mathbf{e}_i)$ which, when applied to a state $\mathbf{e}_i \in \Psi_i$, forces the trajectory of the state of the system to reach the terminal set Ω_i .

Theorem 1. *Suppose that for every $i \in \mathcal{V}$:*

- (1) *Assumptions 1-7 hold;*
- (2) *A solution to FHOCP (9a)-(9d) is feasible at time $t = 0$ with feasible initial conditions, as defined in Definition 6;*
- (3) *The upper bound \bar{w}_i of the disturbance \mathbf{w}_i satisfies the following:*

$$\bar{w}_i \leq \frac{\varepsilon_{\Psi_i} - \varepsilon_{\Omega_i}}{\frac{L_{V_i}}{L_{g_i}}(e^{L_{g_i}h} - 1)e^{L_{g_i}(T_p-h)}}, \quad (15)$$

for all $t \in \mathbb{R}_{\geq 0}$.

Then the closed loop trajectories of the system (6), under the control input (11) which is the outcome of the FHOCP (9a)-(9d), converge to the set Ω_i , as $t \rightarrow \infty$ and are ultimately bounded there, for every $i \in \mathcal{V}$.

Proof. The proof of the above theorem consists of two parts: in the first, recursive feasibility is established, that is, initial feasibility is shown to imply subsequent feasibility; in the second, and based on the first part, it is shown that the error state $\mathbf{e}_i(t)$ reaches the terminal set Ω_i and is trapped there. The feasibility analysis can be found in Appendix H. The convergence analysis can be found in Appendix I. \square

Remark 5. Inequality (15) gives an upper bound of the disturbance that the proposed methodology can handle. Disturbances exceeding this bound cannot guarantee the feasibility of Theorem 1.

Remark 6. Due to the existence of disturbances, the position and orientation error of each agent cannot be made to become arbitrarily close to zero, and therefore $\lim_{t \rightarrow \infty} \|\mathbf{e}_i(t)\|$ cannot converge to zero. However, if the conditions of Theorem 2 hold, then this error can be bounded above by the quantity $\sqrt{\varepsilon_{\Omega_i}/\lambda_{\max}(\mathbf{P}_i)}$ (since the trajectory of the error is trapped in the terminal set, this means that $V(\mathbf{e}_i) = \mathbf{e}_i^\top \mathbf{P}_i \mathbf{e}_i \leq \varepsilon_{\Omega_i}$).

Remark 7. In sampled-data Model Predictive Control, the solution to the optimization problem is the input that is implemented on the continuous time system (6). However, the solution of the FHOCP (9c)-(9d) is computed in a discrete-time man-

ner. In order to address this, the input is held constant over the time period between successive solutions of the optimization problem using zero-order hold. For more details we refer the reader to [43]. Implementation tools of this approach, which we also have adopted for our simulation experiments (see next section), can be found in [45].

5. Simulation Results

For a simulation scenario, consider $N = 3$ unicycle agents with dynamics: $\dot{\mathbf{z}}_i(t) = \begin{bmatrix} \dot{x}_i(t) \\ \dot{y}_i(t) \\ \dot{\theta}_i(t) \end{bmatrix} = \begin{bmatrix} v_i(t) \cos \theta_i(t) \\ v_i(t) \sin \theta_i(t) \\ \omega_i(t) \end{bmatrix} + w_i(t) \begin{bmatrix} 1 \\ 1 \\ 1 \end{bmatrix}$, $i \in \mathcal{V} = \{1, 2, 3\}$, where: $\mathbf{z}_i = [x_i, y_i, \theta_i]^\top$, $f_i(\mathbf{z}_i, \mathbf{u}_i) = [v_i \cos \theta_i, v_i \sin \theta_i, \omega_i]^\top$, $\mathbf{u}_i = [v_i, \omega_i]^\top$, $w_i = \bar{w}_i \sin(2t)$, with $\bar{w}_i = 0.1$. For the control inputs we set $\bar{u}_i = 8\sqrt{2}$. The radius of the agents is $r_i = 0.5$. The sensing range of all agents is $d_i = 4r_i = 2.0$. Their obstacle-detection range is set to $b_i = 4.0$. We set $\varepsilon = 0.01$, where ε is the parameter of the constraint set \mathcal{Z}_i . The neighboring sets are set to $\mathcal{N}_1 = \{2, 3\}$, $\mathcal{N}_2 = \mathcal{N}_3 = \{1\}$. Agent 3 is chosen to execute motions first, then agent 1, followed by agent 2. The agents' initial positions are $\mathbf{z}_1 = [-6, 3.5, 0]^\top$, $\mathbf{z}_2 = [-6, 2.3, 0]^\top$ and $\mathbf{z}_3 = [-6, 4.7, 0]^\top$. Their desired configurations in steady-state are $\mathbf{z}_{1,\text{des}} = [6, 3.5, 0]^\top$, $\mathbf{z}_{2,\text{des}} = [6, 2.3, 0]^\top$ and $\mathbf{z}_{3,\text{des}} = [6, 4.7, 0]^\top$. In the workspace, we place 2 obstacles with centers at points $[0, 2.0]^\top$ and $[0, 5.5]^\top$, respectively. The obstacles' radii are $r_{o_\ell} = 1.0$, $\ell \in \mathcal{L} = \{1, 2\}$. The matrices \mathbf{Q}_i , \mathbf{R}_i , \mathbf{P}_i are set to $\mathbf{Q}_i = 0.5(I_3 + 0.5\uparrow_3)$, $\mathbf{R}_i = 0.005[5 \ 0; 0 \ 1]$ and $\mathbf{P}_i = 0.3(I_3 + 0.5\uparrow_3)$, where \uparrow_N is a $N \times N$ matrix whose elements are randomly chosen between the values 0.0 and 1.0. The maximum eigenvalue of matrix \mathbf{P}_i was found to be $\lambda_{\max}(\mathbf{P}_i) = 0.4710$. The sampling time is $h = 0.1$ sec, the time-horizon is $T_p = 0.6$ sec, and the total execution time given is 10 sec. Furthermore, we set: $L_{f_i} = 8.5883$, $L_{V_i} = 0.0471$, $\varepsilon_{\Psi_i} = 0.0582$ and $\varepsilon_{\Omega_i} = 0.0035$ for all $i \in \mathcal{V}$.

The frames of the evolution of the trajectories of the three agents in the $x - y$ plane are depicted in Figure 7; Figure 8 depicts the evolution of the error states' 2-norms of the agents; Figure 9 depicts the evolution of the error states' 2-norms of the agents in greater detail; Figure 10 shows the evolution of the distances between the neighboring agents; Figure 11 and Figure 12 depict the distance between the agents and the obstacle 1 and 2, respectively; Figure 13 shows the input signals directing the agents through time; Figure 14 shows the evolution of the \mathbf{P} -norms of the errors of the three agents through time (i.e, $\mathbf{e}_i(t)^\top \mathbf{P}_i \mathbf{e}_i(t)$, $i \in \{1, 2, 3\}$), and Figure 15 shows the evolution of the \mathbf{P} -norms of the errors of the three agents through time in more detail, and for an extended execution time of $t = 100$ seconds, without altering the rest of the simulation variables. Notably, the trajectories of the three agents are trapped inside the terminal set once they enter it, since the magnitudes of their \mathbf{P} -weighted error norms do not exceed the value of ε_{Ω_i} once they fall below it. Furthermore, it can be observed that all agents reach their desired goal by satisfying all the constraints imposed by Problem 1. The simulation was performed in MATLAB R2015a Environment utilizing the NMPC optimization routine provided in [45]. The simulation takes 1340 sec on a desktop with 8 cores, 3.60GHz CPU and 16GB of RAM.

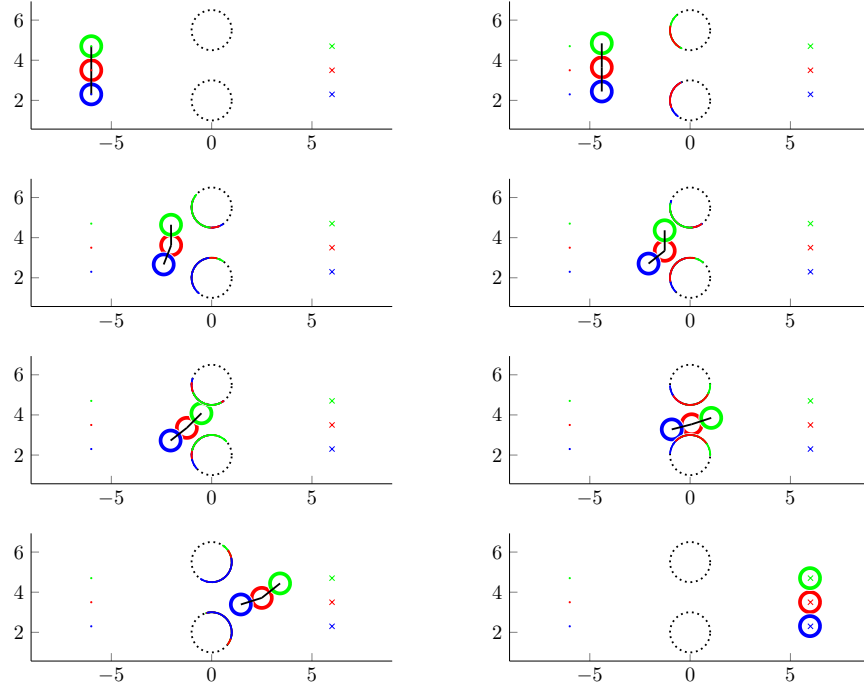


Figure 7.: The trajectories of the three agents in the $x - y$ plane. Agent 1 is in red, agent 2 in blue and agent 3 in green. Agent 3 executes its motions first, followed by agent 1 and then agent 2. A faint black line connects agents deemed neighbors. A point on the circumference of the obstacles is black and dotted when it is not visible by an agent; otherwise it is colored in accordance with which agent it is visible. Mark X marks the desired configurations.

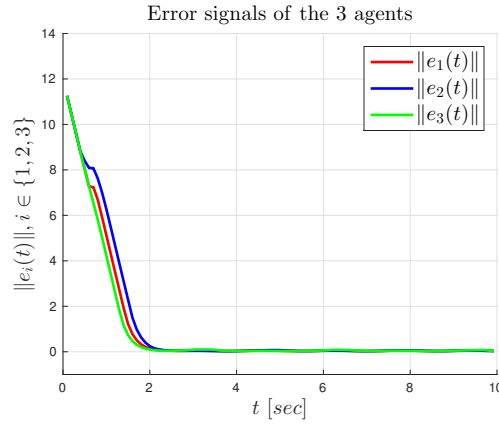


Figure 8.: The evolution of the 2-norms of the error signals of the three agents over time.

6. Conclusions

This paper addresses the problem of stabilizing a multiple rigid-bodies system under constraints relating to the maintenance of connectivity between agents, the aversion of collision among agents and between agents and stationary obstacles within their working environment, and constraints regarding their states and control inputs. The proposed framework is a Decentralized Nonlinear Model Predictive Control scheme. Simulation results verify the controller efficiency of the proposed framework. Future efforts will be devoted to reduce the communication burden between the agents by introducing event-triggered communication controllers.

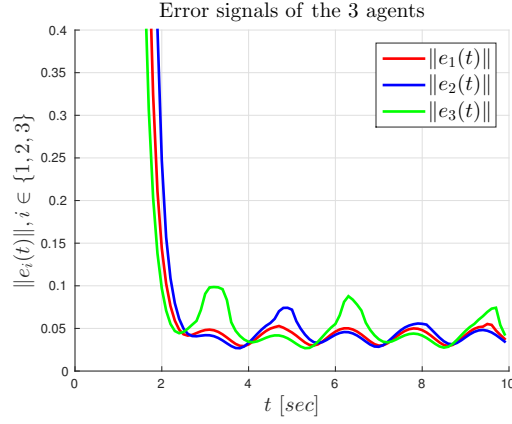


Figure 9.: The evolution of the 2–norms of the error signals of the three agents over time, in greater detail.

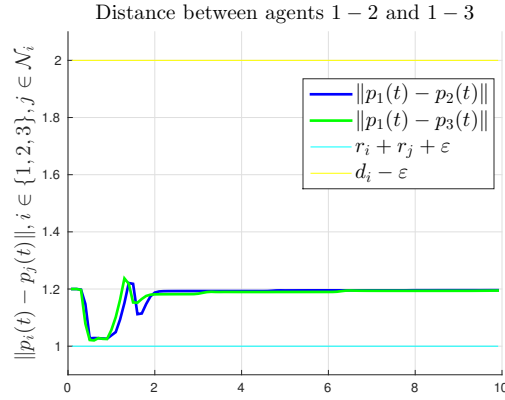


Figure 10.: The distance between agents 1 – 2 and 1 – 3 over time. The maximum and the minimum allowed distances are $d_i - \varepsilon = 1.99$ and $r_i + r_j + \varepsilon = 1.01$, respectively for every $i \in \mathcal{V}$, $j \in \mathcal{N}_i$.

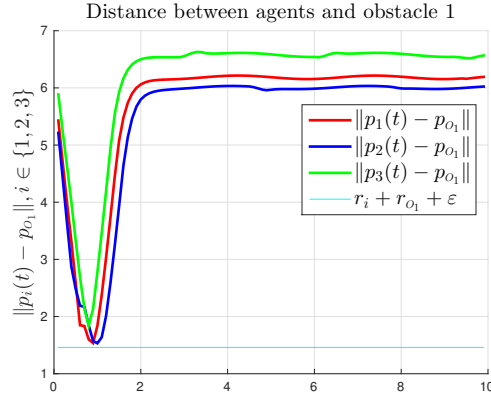


Figure 11.: The distance between the agents and obstacle 1 over time. The minimum allowed distance is $r_i + r_{o_1} + \varepsilon = 1.51$.

Disclosure Statement

No potential conflict of interest was reported by the authors.

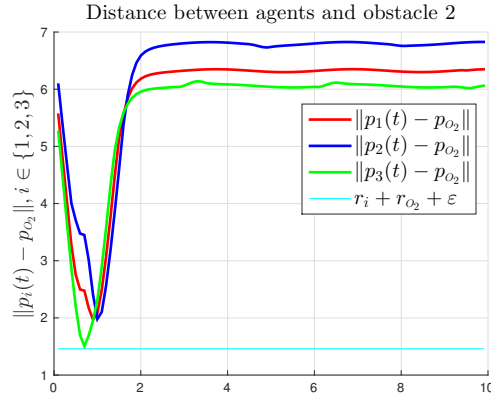


Figure 12.: The distance between the agents and obstacle 2 over time. The minimum allowed distance is $r_i + r_{o_2} + \varepsilon = 1.51$.

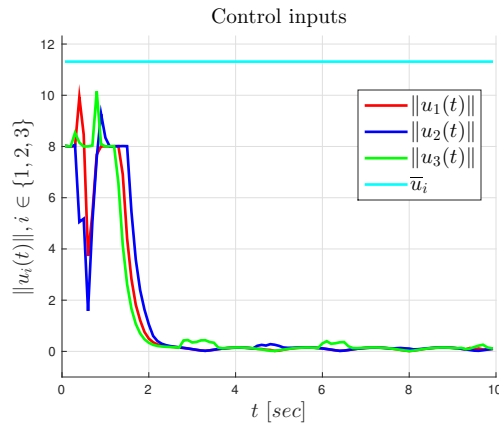


Figure 13.: The norms of control input-signals directing the three agents over time. Their value is upper-bounded by $\bar{u}_i = 15$, as \bar{u}_i defined in (3).

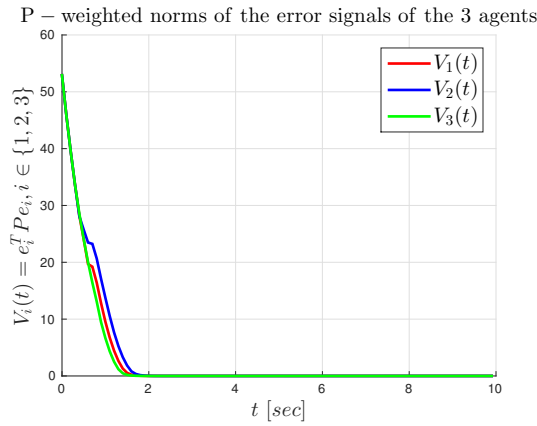


Figure 14.: The P -weighted norms of the errors of the three agents over time. $V_i(t), i = 1, 2, 3$ decreases monotonically until it reaches a value below the threshold ε_{Ω_i} .

Funding

This work was supported by the H2020 ERC Starting Grant BUCOPHSYS, the EU H2020 Co4Robots project, the Swedish Foundation for Strategic Research (SSF),

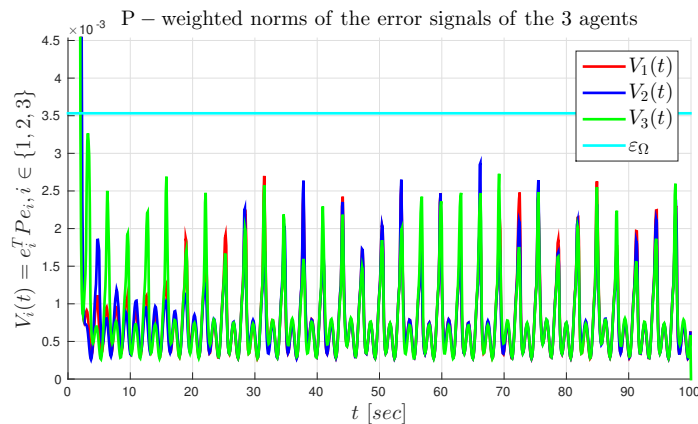


Figure 15.: The \mathbf{P} -weighted norms of the errors of the three agents over an extended execution time of 100 seconds. Notice that the magnitudes of V_i do not exceed the threshold $\varepsilon_{\Omega_i}, i = 1, 2, 3$ as guaranteed by the control strategy. The periodic rise and fall of the magnitudes of V_i is due to the periodic nature of the disturbance.

the Swedish Research Council (VR) and the Knut och Alice Wallenberg Foundation (KAW).

References

- [1] W. Ren and R. Beard. Consensus Seeking in Multi-agent Systems under Dynamically Changing Interaction Topologies. *IEEE Transactions on Automatic Control (TAC)*, 50(5):655–661, 2005.
- [2] R. Olfati-Saber and R. Murray. Consensus Problems in Networks of Agents with Switching Topology and Time-Delays. *IEEE Transactions on Automatic Control (TAC)*, 49(9):1520–1533, 2004.
- [3] A. Jadbabaie, J. Lin, and S. Morse. Coordination of Groups of Mobile Autonomous Agents Using Nearest Neighbor Rules. *IEEE Transactions on Automatic Control (TAC)*, 48(6):988–1001, 2003.
- [4] H. Tanner, A. Jadbabaie, and G. Pappas. Flocking in Fixed and Switching Networks. *IEEE Transactions on Automatic Control (TAC)*, 52(5):863–868, 2007.
- [5] M. Egerstedt and X. Hu. Formation Constrained Multi-Agent Control. *IEEE Transactions on Robotics and Automation (TRA)*, 17(6):947–951, 2001.
- [6] K. Oh, M. Park, and H. Ahn. A Survey of Multi-Agent Formation Control. *Automatica*, 53:424–440, 2015.
- [7] B. Anderson, C. Yu, B. Fidan, and J. Hendrickx. Rigid Graph Control Architectures for Autonomous Formations. *IEEE Control Systems*, 28:48–63, 2008.
- [8] M. Cao, S. Morse, C. Yu, B. Anderson, and S. Dasgupta. Maintaining a Directed, Triangular Formation of Mobile Autonomous Agents. *Communications in Information and Systems*, 11(1):1, 2011.
- [9] C. K. Verginis, A. Nikou, and D. V. Dimarogonas. Position and Orientation Based Formation Control of Multiple Rigid Bodies with Collision Avoidance and Connectivity Maintenance. *56th IEEE Conference on Decision and Control (CDC), Melbourne, Australia, 2017*.
- [10] A. Nikou, C. K. Verginis, and D. V. Dimarogonas. Robust Distance-Based Formation Control of Multiple Rigid Bodies with Orientation Alignment. *20th World*

- Congress of the International Federation of Automatic Control (IFAC WC), Toulouse, France, 2017.*
- [11] C. K. Verginis, A. Nikou, and D. V. Dimarogonas. Robust Formation Control in SE(3) for Tree Graph Structures with Prescribed Transient and Steady State Performance. *Automatica (Under Review)*, 2018.
 - [12] M. Ji and M. Egerstedt. Distributed Coordination Control of Multi-Agent Systems While Preserving Connectedness. *IEEE Transactions on Robotics (TRO)*, 23(4):693–703, 2007.
 - [13] M. Zavlanos and G. Pappas. Distributed Connectivity Control of Mobile Networks. *IEEE Transactions on Robotics (TRO)*, 24(6):1416–1428, 2008.
 - [14] A. Nikou, S. Heshmati-alamdari, C. K. Verginis, and D. V. Dimarogonas. Decentralized Abstractions and Timed Constrained Planning of a General Class of Coupled Multi-Agent Systems. *56th IEEE Conference on Decision and Control (CDC), Melbourne, Australia, 2017.*
 - [15] D. V. Dimarogonas, S. Loizou, K. Kyriakopoulos, and M. Zavlanos. A Feedback Stabilization and Collision Avoidance Scheme for Multiple Independent Non-Point Agents. *Automatica*, 42(2):229–243, 2006.
 - [16] A. Nikou, C. K. Verginis, S. Heshmati-alamdari, and D. V. Dimarogonas. A Nonlinear Model Predictive Control Scheme for Cooperative Manipulation with Singularity and Collision Avoidance. *25th IEEE Mediterranean Conference on Control and Automation (MED), Valletta, Malta, 2017.*
 - [17] C. K. Verginis, A. Nikou, and D. V. Dimarogonas. Communication Based Decentralized Cooperative Object Transportation Using Nonlinear Model Predictive Control. *IEEE European Control Conference (ECC), Limassol, Cyprus, 2018.*
 - [18] L. Makarek and D. Gillet. Decentralized Coordination of Autonomous Vehicles at Intersections. *18th World Congress of International Federation of Automatic Control (IFAC WC)*, 44(1):13046–13051, 2011.
 - [19] D. Koditschek and E. Rimon. Robot Navigation Functions on Manifolds with Boundary. *Advances in Applied Mathematics*, 11(4):412–442, 1990.
 - [20] D. Panagou. A Distributed Feedback Motion Planning Protocol for Multiple Unicycle Agents of Different Classes. *IEEE Transactions on Automatic Control (TAC)*, 62(3):1178–1193, 2017.
 - [21] J. Baras, X. Tan, and P. Hovareshti. Decentralized Control of Autonomous Vehicles. *42nd IEEE Conference on Decision and Control (CDC)*, 2:1532–1537, 2003.
 - [22] H. Roozbehani, S. Rudaz, and D. Gillet. A Hamilton-Jacobi Formulation for Cooperative Control of Multi-Agent Systems. *IEEE International Conference on Systems, Man, and Cybernetics (SMC)*, pages 4813–4818, 2009.
 - [23] Savvas G Loizou. The Multi-Agent Navigation Transformation: Tuning-Free Multi-Robot Navigation. *Robotics: Science and Systems*, 2014.
 - [24] W. Dunbar and R. Murray. Distributed Receding Horizon Control for Multi-Vehicle Formation Stabilization. *Automatica*, 42(4):549 – 558, 2006.
 - [25] A. Rucco, P. Aguiar, F. Fontes, F. Pereira, and J. B. Sousa. A Model Predictive Control-Based Architecture for Cooperative Path-Following of Multiple Unmanned Aerial Vehicles. *Developments in Model-Based Optimization and Control*, pages 141–160, 2015.
 - [26] D. H. Shim, H. J. Kim, and S. Sastry. Decentralized Nonlinear Model Predictive Control of Multiple Flying Robots. *42nd IEEE International Conference on Decision and Control (CDC)*, 4:3621–3626 vol.4, 2003.
 - [27] H. Fukushima, K. Kon, and F. Matsuno. Distributed Model Predictive Control

- for Multi-Vehicle Formation with Collision Avoidance Constraints. *44th IEEE Conference on Decision and Control (CDC)*, pages 5480–5485, 2005.
- [28] T. Keviczky, F. Borrelli, K. Fregene, D. Godbole, and G. J. Balas. Decentralized Receding Horizon Control and Coordination of Autonomous Vehicle Formations. *IEEE Transactions on Control Systems Technology (TCST)*, 16(1):19–33, 2008.
- [29] T. Keviczky, F. Borrelli, and G. Balas. Decentralized Receding Horizon Control for Large Scale Dynamically Decoupled Systems. *Automatica*, 42(12):2105–2115, 2006.
- [30] E. Franco, L. Magni, T. Parisini, M. M. Polycarpou, and D. M. Raimondo. Cooperative Constrained Control of Distributed Agents with Nonlinear Dynamics and Delayed Information Exchange: A Stabilizing Receding-Horizon Approach. *IEEE Transactions on Automatic Control (TAC)*, 53(1):324–338, 2008.
- [31] A. Richards and J. How. A Decentralized Algorithm for Robust Constrained Model Predictive Control. *2004 American Control Conference (ACC)*, 5:4261–4266 vol.5, 2004.
- [32] A. Richards and J. How. Decentralized Model Predictive Control of Cooperating UAVs. *43rd IEEE Conference on Decision and Control (CDC)*, 4:4286–4291 Vol.4, 2004.
- [33] A. Filotheou, A. Nikou, and D. V. Dimarogonas. Decentralized Control of Uncertain Multi-Agent Systems with Connectivity Maintenance and Collision Avoidance. *IEEE European Control Conference (ECC)*, Limassol, Cyprus, 2018.
- [34] H. K. Khalil. *Nonlinear Systems*. Prentice Hall, 2002.
- [35] H. Marquez. *Nonlinear Control Systems: Analysis and Design*. Wiley, 2003.
- [36] E. Sontag and Y. Wang. On Characterizations of the Input-to-State Stability Property. *System and Control Letters*, 24(5):351–359, April 1995.
- [37] D. Mayne, J. Rawlings, C. Rao, and P. Scokaert. Constrained Model Predictive Control: Stability and Optimality. *Automatica*, 36(6):789 – 814, 2000.
- [38] K. Oliveira and M. Morari. Contractive Model Predictive Control for Constrained Nonlinear Systems. *IEEE Transactions on Automatic Control (TAC)*, 45(6):1053–1071, 2000.
- [39] H. Chen and F. Allgöwer. A Quasi-Infinite Horizon Nonlinear Model Predictive Control Scheme with Guaranteed Stability. *Automatica*, 34(10):1205–1217, 1998.
- [40] B. Kouvaritakis and M. Cannon. *Nonlinear Predictive Control: Theory and Practice*. Number 61. Iet, 2001.
- [41] E. Camacho and C. Bordons. *Nonlinear Model Predictive Control: An Introductory Review*. pages 1–16, 2007.
- [42] F. Fontes. A General Framework to Design Stabilizing Nonlinear Model Predictive Controllers. *Systems and Control Letters*, 42(2):127–143, 2001.
- [43] R. Findeisen, L. Imsland, F. Allgöwer, and B. Foss. Towards a Sampled-Data Theory for Nonlinear Model Predictive Control. *New Trends in Nonlinear Dynamics and Control and their Applications*, pages 295–311, 2003.
- [44] J. Frasch, A. Gray, M. Zanon, H. Ferreau, S. Sager, F. Borrelli, and M. Diehl. An Auto-Generated Nonlinear MPC Algorithm for Real-Time Obstacle Cvoidance of Ground Vehicles. *IEEE European Control Conference (ECC)*, 2013.
- [45] L. Grüne and J. Pannek. *Nonlinear Model Predictive Control: Theory and Algorithms*. Springer International Publishing, 2016.
- [46] D. Marruedo, T. Alamo, and E. Camacho. Input-to-State Stable MPC for Constrained Discrete-Time Nonlinear Systems with Bounded Additive Uncertainties. *41st IEEE Conference on Decision and Control (CDC)*, 4:4619–4624 vol.4, 2002.
- [47] F. Fontes, L. Magni, and E. Gyurkovics. *Sampled-Data Model Predictive Control*

- for *Nonlinear Time-Varying Systems: Stability and Robustness*. Springer Berlin Heidelberg, Berlin, Heidelberg, 2007.
- [48] A. Eqtami, D. V. Dimarogonas, and K. Kyriakopoulos. Novel Event-Triggered Strategies for Model Predictive Controllers. *IEEE Conference on Decision and Control (CDC)*, pages 3392–3397, 2011.
- [49] H. Michalska and D. Q. Mayne. Robust Receding Horizon Control of Constrained Nonlinear Systems. *IEEE Transactions on Automatic Control (TAC)*, 38(11):1623–1633, 1993.
- [50] R. Findeisen, L. Imstrand, F. Allgöwer, and B. Foss. State and Output Feedback Nonlinear Model Predictive Control: An Overview. *European Journal of Control (EJC)*, 9(2):190–206, 2003.
- [51] I. Kolmanovsky and E. Gilbert. Theory and Computation of Disturbance Invariant Sets for Discrete-Time Linear Systems. *Mathematical Problems in Engineering*, 4(4):317–367, 1998.
- [52] R. Schneider. *Minkowski Addition*. Encyclopedia of Mathematics and its Applications. Cambridge University Press, 2013.

Appendix A. Proof of Property 1

Consider the vectors $\mathbf{u}, \mathbf{v}, \mathbf{w}, \mathbf{x} \in \mathbb{R}^n$. According to Definition 2, we have that: $\mathcal{S}_1 \ominus \mathcal{S}_2 = \{\mathbf{u} \in \mathbb{R}^n : \mathbf{u} + \mathbf{v} \in \mathcal{S}_1, \forall \mathbf{v} \in \mathcal{S}_2\}$, $\mathcal{S}_2 \ominus \mathcal{S}_3 = \{\mathbf{w} \in \mathbb{R}^n : \mathbf{w} + \mathbf{x} \in \mathcal{S}_2, \forall \mathbf{x} \in \mathcal{S}_3\}$. Then, by adding the aforementioned sets according to Definition 1 we get:

$$\begin{aligned} & (\mathcal{S}_1 \ominus \mathcal{S}_2) \oplus (\mathcal{S}_2 \ominus \mathcal{S}_3) \\ &= \{\mathbf{u} + \mathbf{w} \in \mathbb{R}^n : \mathbf{u} + \mathbf{v} \in \mathcal{S}_1 \text{ and } \mathbf{w} + \mathbf{x} \in \mathcal{S}_2, \forall \mathbf{v} \in \mathcal{S}_2, \forall \mathbf{x} \in \mathcal{S}_3\} \\ &= \{\mathbf{u} + \mathbf{w} \in \mathbb{R}^n : \mathbf{u} + \mathbf{v} + \mathbf{w} + \mathbf{x} \in (\mathcal{S}_1 \oplus \mathcal{S}_2), \forall \mathbf{v} + \mathbf{x} \in (\mathcal{S}_2 \oplus \mathcal{S}_3)\}. \end{aligned} \quad (\text{A1})$$

By setting $\mathbf{s}_1 = \mathbf{u} + \mathbf{w} \in \mathbb{R}^n$, $\mathbf{s}_2 = \mathbf{v} + \mathbf{x} \in \mathbb{R}^n$ and employing Definition 2, (A1) becomes: $(\mathcal{S}_1 \ominus \mathcal{S}_2) \oplus (\mathcal{S}_2 \ominus \mathcal{S}_3) = \{\mathbf{s}_1 \in \mathbb{R}^n : \mathbf{s}_1 + \mathbf{s}_2 \in (\mathcal{S}_1 \oplus \mathcal{S}_2), \forall \mathbf{s}_2 \in (\mathcal{S}_2 \oplus \mathcal{S}_3)\} = (\mathcal{S}_1 \oplus \mathcal{S}_2) \ominus (\mathcal{S}_2 \oplus \mathcal{S}_3)$, which concludes the proof. \square

Appendix B. Proof of Property 2

By setting $\mathbf{z} = \mathbf{e} + \mathbf{z}_{\text{des}}$, $\mathbf{z}' = \mathbf{e}' + \mathbf{z}_{\text{des}}$ in (4) we get: $\|f_i(\mathbf{e} + \mathbf{z}_{\text{des}}, \mathbf{u}) - f_i(\mathbf{e}' + \mathbf{z}_{\text{des}}, \mathbf{u})\| \leq L_{f_i} \|\mathbf{e} + \mathbf{z}_{\text{des}} - \mathbf{e}' - \mathbf{z}_{\text{des}}\|$. By using (7b), the latter becomes: $\|g_i(\mathbf{e}, \mathbf{u}) - g_i(\mathbf{e}', \mathbf{u})\| \leq L_{g_i} \|\mathbf{e} - \mathbf{e}'\|$, where $L_{g_i} = L_{f_i}$, which leads to the conclusion of the proof. \square

Appendix C. Proof of Lemma 1

By invoking the fact that:

$$\lambda_{\min}(\mathbf{P}) \|\mathbf{y}\|^2 \leq \mathbf{y}^\top \mathbf{P} \mathbf{y} \leq \lambda_{\max}(\mathbf{P}) \|\mathbf{y}\|^2, \forall \mathbf{y} \in \mathbb{R}^n, \mathbf{P} \in \mathbb{R}^{n \times n}, \mathbf{P} = \mathbf{P}^\top > 0, \quad (\text{C1})$$

we have: $\mathbf{e}_i^\top \mathbf{Q}_i \mathbf{e}_i + \mathbf{u}_i^\top \mathbf{R}_i \mathbf{u}_i \leq \max\{\lambda_{\max}(\mathbf{Q}_i), \lambda_{\max}(\mathbf{R}_i)\} \|\boldsymbol{\eta}_i\|^2$, and: $\mathbf{e}_i^\top \mathbf{Q}_i \mathbf{e}_i + \mathbf{u}_i^\top \mathbf{R}_i \mathbf{u}_i \geq \min\{\lambda_{\min}(\mathbf{Q}_i), \lambda_{\min}(\mathbf{R}_i)\} \|\boldsymbol{\eta}_i\|^2$, where $\boldsymbol{\eta}_i = [\mathbf{e}_i^\top, \mathbf{u}_i^\top]^\top$ and $i \in \mathcal{V}$. By defining the \mathcal{K}_∞ functions $\alpha_1, \alpha_2 : \mathbb{R}_{\geq 0} \rightarrow \mathbb{R}_{\geq 0}$: $\alpha_1(y) \triangleq \min\{\lambda_{\min}(\mathbf{Q}_i), \lambda_{\min}(\mathbf{R}_i)\} \|y\|^2$,

$\alpha_2(y) \triangleq \max\{\lambda_{\max}(\mathbf{Q}_i), \lambda_{\max}(\mathbf{R}_i)\} \|y\|^2$, we get $\alpha_1(\|\boldsymbol{\eta}_i\|) \leq F_i(\mathbf{e}_i, \mathbf{u}_i) \leq \alpha_2(\|\boldsymbol{\eta}_i\|)$. \square

Appendix D. Proof of Lemma 2

For every $\mathbf{e}_i, \mathbf{e}'_i \in \mathcal{E}_i$, and $\mathbf{u}_i \in \mathcal{U}_i$ it holds that:

$$\begin{aligned} |F_i(\mathbf{e}_i, \mathbf{u}_i) - F_i(\mathbf{e}'_i, \mathbf{u}_i)| &= |\mathbf{e}_i^\top \mathbf{Q}_i \mathbf{e}_i + \mathbf{u}_i^\top \mathbf{R}_i \mathbf{u}_i - (\mathbf{e}'_i)^\top \mathbf{Q}_i \mathbf{e}'_i - \mathbf{u}_i^\top \mathbf{R}_i \mathbf{u}_i| \\ &\leq |\mathbf{e}_i^\top \mathbf{Q}_i (\mathbf{e}_i - \mathbf{e}'_i)| + |(\mathbf{e}'_i)^\top \mathbf{Q}_i (\mathbf{e}_i - \mathbf{e}'_i)|. \end{aligned} \quad (\text{D1})$$

By employing the property that: $|\mathbf{e}_i^\top \mathbf{Q}_i \mathbf{e}'_i| \leq \|\mathbf{e}_i\| \|\mathbf{Q}_i \mathbf{e}'_i\| \leq \|\mathbf{Q}_i\| \|\mathbf{e}_i\| \|\mathbf{e}'_i\| \leq \sigma_{\max}(\mathbf{Q}_i) \|\mathbf{e}_i\| \|\mathbf{e}'_i\|$, (D1) is written as: $|F_i(\mathbf{e}_i, \mathbf{u}_i) - F_i(\mathbf{e}'_i, \mathbf{u}_i)| \leq \sigma_{\max}(\mathbf{Q}_i) \|\mathbf{e}_i\| \|\mathbf{e}_i - \mathbf{e}'_i\| + \sigma_{\max}(\mathbf{Q}_i) \|\mathbf{e}'_i\| \|\mathbf{e}_i - \mathbf{e}'_i\| \leq \left[2\sigma_{\max}(\mathbf{Q}_i) \sup_{\mathbf{e}_i \in \mathcal{E}_i} \|\mathbf{e}_i\| \right] \|\mathbf{e}_i - \mathbf{e}'_i\| = L_{F_i} \|\mathbf{e}_i - \mathbf{e}'_i\|$. \square

Appendix E. Proof of Lemma 3

By employing Property 3 and substituting $\tau \equiv t_k$ and $s \equiv t_k + s$ in (12a), (12b) yields: $\mathbf{e}_i(t_k + s; \bar{\mathbf{u}}_i(\cdot; \mathbf{e}_i(t_k)), \mathbf{e}_i(t_k)) = \mathbf{e}_i(t_k) + \int_{t_k}^{t_k+s} g_i(\mathbf{e}_i(s'; \mathbf{e}_i(t_k)), \bar{\mathbf{u}}_i(s')) ds' + \int_{t_k}^{t_k+s} \mathbf{w}_i(\cdot, s') ds'$, $\bar{\mathbf{e}}_i(t_k + s; \bar{\mathbf{u}}_i(\cdot; \mathbf{e}_i(t_k)), \mathbf{e}_i(t_k)) = \mathbf{e}_i(t_k) + \int_{t_k}^{t_k+s} g_i(\bar{\mathbf{e}}_i(s'; \mathbf{e}_i(t_k)), \bar{\mathbf{u}}_i(s')) ds'$, respectively. Subtracting the latter from the former and taking norms on both sides yields: $\left\| \mathbf{e}_i(t_k + s; \bar{\mathbf{u}}_i(\cdot; \mathbf{e}_i(t_k)), \mathbf{e}_i(t_k)) - \bar{\mathbf{e}}_i(t_k + s; \bar{\mathbf{u}}_i(\cdot; \mathbf{e}_i(t_k)), \mathbf{e}_i(t_k)) \right\| = \left\| \int_{t_k}^{t_k+s} g_i(\mathbf{e}_i(s'; \mathbf{e}_i(t_k)), \bar{\mathbf{u}}_i(s')) ds' - \int_{t_k}^{t_k+s} g_i(\bar{\mathbf{e}}_i(s'; \mathbf{e}_i(t_k)), \bar{\mathbf{u}}_i(s')) ds' + \int_{t_k}^{t_k+s} \mathbf{w}_i(\cdot, s') ds' \right\| \leq L_{g_i} \int_{t_k}^{t_k+s} \left\| \mathbf{e}_i(s; \bar{\mathbf{u}}_i(\cdot; \mathbf{e}_i(t)), \mathbf{e}_i(t)) - \bar{\mathbf{e}}_i(s; \bar{\mathbf{u}}_i(\cdot; \mathbf{e}_i(t)), \mathbf{e}_i(t)) \right\| ds + s \bar{w}_i$, since, according to Property 2, g_i is locally Lipschitz continuous in $\mathcal{E}_i \times \mathcal{U}_i$ with Lipschitz constant L_{g_i} . Then, we get: $\left\| \mathbf{e}_i(t_k + s; \bar{\mathbf{u}}_i(\cdot; \mathbf{e}_i(t_k)), \mathbf{e}_i(t_k)) - \bar{\mathbf{e}}_i(t_k + s; \bar{\mathbf{u}}_i(\cdot; \mathbf{e}_i(t_k)), \mathbf{e}_i(t_k)) \right\| \leq s \bar{w}_i + L_{g_i} \int_0^s \left\| \mathbf{e}_i(t_k + s'; \bar{\mathbf{u}}_i(\cdot; \mathbf{e}_i(t_k)), \mathbf{e}_i(t_k)) - \bar{\mathbf{e}}_i(t_k + s'; \bar{\mathbf{u}}_i(\cdot; \mathbf{e}_i(t_k)), \mathbf{e}_i(t_k)) \right\| ds'$. By applying the Grönwall-Bellman inequality (see [34, Appendix A]) we get: $\left\| \mathbf{e}_i(t_k + s; \bar{\mathbf{u}}_i(\cdot; \mathbf{e}_i(t_k)), \mathbf{e}_i(t_k)) - \bar{\mathbf{e}}_i(t_k + s; \bar{\mathbf{u}}_i(\cdot; \mathbf{e}_i(t_k)), \mathbf{e}_i(t_k)) \right\| \leq \frac{\bar{w}_i}{L_{g_i}} (e^{L_{g_i} s} - 1)$. \square

Appendix F. Proof of Property 4

Let us define the function $\zeta_i : \mathbb{R}_{\geq 0} \rightarrow \mathcal{M} \times \mathbb{R}^6$ as: $\zeta_i(s) \triangleq \mathbf{e}_i(s) - \bar{\mathbf{e}}_i(s; \mathbf{u}_i(s; \mathbf{e}_i(t_k)), \mathbf{e}_i(t_k))$, for $s \in [t_k, t_k + T_p]$. According to Lemma 3 we have that: $\|\zeta_i(s)\| = \|\mathbf{e}_i(s) - \bar{\mathbf{e}}_i(s; \mathbf{u}_i(s; \mathbf{e}_i(t_k)), \mathbf{e}_i(t_k))\| \leq \frac{\bar{w}_i}{L_{g_i}} (e^{L_{g_i}(s-t)} - 1)$, $s \in [t_k, t_k + T_p]$, which means that $\zeta_i(s) \in \mathcal{X}_{i,s-t}$. Now we have that: $\bar{\mathbf{e}}_i(s; \mathbf{u}_i(\cdot, \mathbf{e}_i(t_k)), \mathbf{e}_i(t_k)) \in \mathcal{E}_i \ominus \mathcal{X}_{i,s-t_k}$. Then, it holds that: $\zeta_i(s) + \bar{\mathbf{e}}_i(s; \mathbf{u}_i(s; \mathbf{e}_i(t_k)), \mathbf{e}_i(t_k)) \in (\mathcal{E}_i \ominus \mathcal{X}_{i,s-t_k}) \oplus \mathcal{X}_{i,s-t_k}$,

or: $\mathbf{e}_i(s) \in (\mathcal{E}_i \ominus \mathcal{X}_{i,s-t_k}) \oplus \mathcal{X}_{i,s-t_k}$. Theorem 2.1 (ii) from [51] states that for every $U, V \subseteq \mathbb{R}^n$ it holds that: $(U \ominus V) \oplus V \subseteq U$. By invoking the latter result we get: $\mathbf{e}_i(s) \in (\mathcal{E}_i \ominus \mathcal{X}_{i,s-t_k}) \oplus \mathcal{X}_{i,s-t_k} \subseteq \mathcal{E}_i \Rightarrow \mathbf{e}_i(s) \in \mathcal{E}_i, s \in [t_k, t_k + T_p]$. \square

Appendix G. Proof of Lemma 4

By invoking (C1) we get: $\lambda_{\min}(\mathbf{P}_i)\|\mathbf{e}_i\|^2 \leq \mathbf{e}_i^\top \mathbf{P}_i \mathbf{e}_i \leq \lambda_{\max}(\mathbf{P}_i)\|\mathbf{e}_i\|^2, \forall \mathbf{e}_i \in \Psi_i, i \in \mathcal{V}$. By defining the \mathcal{K}_∞ functions $\alpha_1, \alpha_2 : \mathbb{R}_{\geq 0} \rightarrow \mathbb{R}_{\geq 0}$: $\alpha_1(y) \triangleq \lambda_{\min}(\mathbf{P}_i)\|y\|^2, \alpha_2(y) \triangleq \lambda_{\max}(\mathbf{P}_i)\|y\|^2$, we get: $\alpha_1(\|\mathbf{e}_i\|) \leq V_i(\mathbf{e}_i) \leq \alpha_2(\|\mathbf{e}_i\|), \forall \mathbf{e}_i \in \Psi_i, i \in \mathcal{V}$. \square

Appendix H. Feasibility Analysis

In this section we will show that there can be constructed an admissible but not necessarily optimal control input according to Definition 7.

Consider a sampling instant t_k for which a solution $\bar{\mathbf{u}}_i^*(\cdot; \mathbf{e}_i(t_k))$ to Problem 1 exists. Suppose now a time instant t_{k+1} such that $t_k < t_{k+1} < t_k + T_p$, and consider that the optimal control signal calculated at t_k is comprised by the following two portions:

$$\bar{\mathbf{u}}_i^*(\cdot; \mathbf{e}_i(t_k)) = \begin{cases} \bar{\mathbf{u}}_i^*(\tau_1; \mathbf{e}_i(t_k)), & \tau_1 \in [t_k, t_{k+1}], \\ \bar{\mathbf{u}}_i^*(\tau_2; \mathbf{e}_i(t_k)), & \tau_2 \in [t_{k+1}, t_k + T_p]. \end{cases} \quad (\text{H1})$$

Both portions are admissible since the calculated optimal control input is admissible, and hence they both conform to the input constraints. As for the resulting predicted states, they satisfy the state constraints, and, crucially:

$$\bar{\mathbf{e}}_i(t_k + T_p; \bar{\mathbf{u}}_i^*(\cdot, \mathbf{e}_i(t_k))) \in \Omega_i. \quad (\text{H2})$$

Furthermore, according to condition (3) of Theorem 1, there exists an admissible (and certainly not guaranteed optimal feedback control) input $\kappa_i \in \mathcal{U}_i$ that renders Ψ_i (and consequently Ω_i) invariant over $[t_k + T_p, t_{k+1} + T_p]$.

Given the above facts, we can construct an admissible input $\tilde{\mathbf{u}}_i(\cdot)$ for time t_{k+1} by sewing together the second portion of (H1) and the admissible input $\kappa_i(\cdot)$:

$$\tilde{\mathbf{u}}_i(\tau) = \begin{cases} \bar{\mathbf{u}}_i^*(\tau; \mathbf{e}_i(t_k)), & \tau \in [t_{k+1}, t_k + T_p], \\ \kappa_i(\bar{\mathbf{e}}_i(\tau; \bar{\mathbf{u}}_i^*(\cdot, \mathbf{e}_i(t_k+1))), & \tau \in (t_k + T_p, t_{k+1} + T_p]. \end{cases} \quad (\text{H3})$$

Applied at time t_{k+1} , $\tilde{\mathbf{u}}_i(\tau)$ is an admissible control input with respect to the input constraints as a composition of admissible control inputs, for all $\tau \in [t_{k+1}, t_{k+1} + T_p]$. What remains to prove is the following two statements:

Statement 1 : $\mathbf{e}_i(t_{k+1} + s; \bar{\mathbf{u}}_i^*(\cdot, \mathbf{e}_i(t_{k+1}))) \in \mathcal{E}_i, \forall s \in [0, T_p]$.

Statement 2 : $\bar{\mathbf{e}}_i(t_{k+1} + T_p; \tilde{\mathbf{u}}_i(\cdot, \mathbf{e}_i(t_{k+1}))) \in \Omega_i$.

Proof of Statement 1 : Initially we have that: $\bar{\mathbf{e}}_i(t_{k+1} + s; \tilde{\mathbf{u}}_i(\cdot, \mathbf{e}_i(t_{k+1}))) \in \mathcal{E}_i \ominus \mathcal{X}_s$, for all $s \in [0, T_p]$. By applying Lemma 3 for $t = t_{k+1} + s$ and $\tau = t_k$ we get $\left\| \mathbf{e}_i(t_{k+1} +$

$s; \bar{\mathbf{u}}_i^*(\cdot, \mathbf{e}_i(t_k)) - \bar{\mathbf{e}}_i(t_{k+1} + s; \bar{\mathbf{u}}_i^*(\cdot, \mathbf{e}_i(t_k))) \Big\| \leq \frac{\bar{w}_i}{L_{g_i}} (e^{L_{g_i}(h+s)} - 1)$, or equivalently: $\mathbf{e}_i(t_{k+1} + s; \bar{\mathbf{u}}_i^*(\cdot, \mathbf{e}_i(t_k)) - \bar{\mathbf{e}}_i(t_{k+1} + s; \bar{\mathbf{u}}_i^*(\cdot, \mathbf{e}_i(t_k))) \in \mathcal{X}_{i,h+s}$. By applying a reasoning identical to the proof of Lemma 3 for $t = t_{k+1}$ (in the model equation) and $t = t_k$ (in the real model equation), and $\tau = s$ we get: $\Big\| \mathbf{e}_i(t_{k+1} + s; \bar{\mathbf{u}}_i^*(\cdot, \mathbf{e}_i(t_k)) - \bar{\mathbf{e}}_i(t_{k+1} + s; \bar{\mathbf{u}}_i^*(\cdot, \mathbf{e}_i(t_{k+1}))) \Big\| \leq \frac{\bar{w}_i}{L_{g_i}} (e^{L_{g_i}s} - 1)$, which translates to: $\mathbf{e}_i(t_{k+1} + s; \bar{\mathbf{u}}_i^*(\cdot, \mathbf{e}_i(t_k)) - \bar{\mathbf{e}}_i(t_{k+1} + s; \bar{\mathbf{u}}_i^*(\cdot, \mathbf{e}_i(t_{k+1}))) \in \mathcal{X}_{i,s}$.

Furthermore, we know that the solution to the optimization problem is feasible at time t_k , which means that: $\bar{\mathbf{e}}_i(t_{k+1} + s; \bar{\mathbf{u}}_i^*(\cdot, \mathbf{e}_i(t_k))) \in \mathcal{E}_i \ominus \mathcal{X}_{i,h+s}$. Let us for sake of readability set: $\mathbf{e}_{i,0} = \mathbf{e}_i(t_{k+1} + s; \bar{\mathbf{u}}_i^*(\cdot, \mathbf{e}_i(t_k)))$, $\bar{\mathbf{e}}_{i,0} = \bar{\mathbf{e}}_i(t_{k+1} + s; \bar{\mathbf{u}}_i^*(\cdot, \mathbf{e}_i(t_k)))$, $\bar{\mathbf{e}}_{i,1} = \bar{\mathbf{e}}_i(t_{k+1} + s; \bar{\mathbf{u}}_i^*(\cdot, \mathbf{e}_i(t_{k+1})))$, and translate the above system of inclusion relations: $\mathbf{e}_{i,0} - \bar{\mathbf{e}}_{i,0} \in \mathcal{X}_{i,h+s}$, $\mathbf{e}_{i,0} - \bar{\mathbf{e}}_{i,1} \in \mathcal{X}_{i,s}$, $\bar{\mathbf{e}}_{i,0} \in \mathcal{E}_i \ominus \mathcal{X}_{i,h+s}$.

First we will focus on the first two relations, and we will derive a result that will combine with the third statement so as to prove that the predicted state will be feasible from t_{k+1} to $t_{k+1} + T_p$. Subtracting the second from the first yields $\bar{\mathbf{e}}_{i,1} - \bar{\mathbf{e}}_{i,0} \in \mathcal{X}_{i,h+s} \ominus \mathcal{X}_{i,s}$. Now we use the third relation $\bar{\mathbf{e}}_{i,0} \in \mathcal{E}_i \ominus \mathcal{X}_{i,h+s}$, along with: $\bar{\mathbf{e}}_{i,1} - \bar{\mathbf{e}}_{i,0} \in \mathcal{X}_{i,h+s} \ominus \mathcal{X}_{i,s}$. Adding the latter to the former yields: $\bar{\mathbf{e}}_{i,1} \in (\mathcal{E}_i \ominus \mathcal{X}_{i,h+s}) \oplus (\mathcal{X}_{i,h+s} \ominus \mathcal{X}_{i,s})$. By using Property 1 we get: $\bar{\mathbf{e}}_{i,1} \in (\mathcal{E}_i \oplus \mathcal{X}_{i,h+s}) \ominus (\mathcal{X}_{i,h+s} \oplus \mathcal{X}_{i,s})$. Using implication ¹ (v) of Theorem 2.1 from [51] yields: $\bar{\mathbf{e}}_{i,1} \in \left((\mathcal{E}_i \oplus \mathcal{X}_{i,h+s}) \ominus \mathcal{X}_{i,h+s} \right) \ominus \mathcal{X}_{i,s}$. Using implication ² (3.1.11) from [52] yields $\bar{\mathbf{e}}_{i,1} \in \mathcal{E}_i \ominus \mathcal{X}_{i,s}$, or equivalently:

$$\bar{\mathbf{e}}_i(t_{k+1} + s; \bar{\mathbf{u}}_i^*(\cdot, \mathbf{e}_i(t_{k+1}))) \in \mathcal{E}_i \ominus \mathcal{X}_{i,s}, \quad \forall s \in [0, T_p]. \quad (\text{H4})$$

By consulting with Property 4, this means that the state of the ‘‘true’’ system does not violate the constraints \mathcal{E}_i over the horizon $[t_{k+1}, t_{k+1} + T_p]$: $\bar{\mathbf{e}}_i(t_{k+1} + s; \bar{\mathbf{u}}_i^*(\cdot, \mathbf{e}_i(t_{k+1}))) \in \mathcal{E}_i \ominus \mathcal{X}_{i,s} \Rightarrow \mathbf{e}_i(t_{k+1} + s; \bar{\mathbf{u}}_i^*(\cdot, \mathbf{e}_i(t_{k+1}))) \in \mathcal{E}_i, \quad \forall s \in [0, T_p]$.

Proof of Statement 3: To prove this statement we begin with:

$$\begin{aligned} & V_i(\bar{\mathbf{e}}_i(t_k + T_p; \bar{\mathbf{u}}_i^*(\cdot, \mathbf{e}_i(t_{k+1})))) - V_i(\bar{\mathbf{e}}_i(t_k + T_p; \bar{\mathbf{u}}_i^*(\cdot, \mathbf{e}_i(t_k)))) \\ & \leq L_{V_i} \left\| \bar{\mathbf{e}}_i(t_k + T_p; \bar{\mathbf{u}}_i^*(\cdot, \mathbf{e}_i(t_{k+1}))) - \bar{\mathbf{e}}_i(t_k + T_p; \bar{\mathbf{u}}_i^*(\cdot, \mathbf{e}_i(t_k))) \right\|. \quad (\text{H5}) \end{aligned}$$

Consulting with Remark 3 we get that the two terms inside the norm are respectively equal to: $\bar{\mathbf{e}}_i(t_k + T_p; \bar{\mathbf{u}}_i^*(\cdot, \mathbf{e}_i(t_{k+1}))) = \mathbf{e}_i(t_{k+1}) + \int_{t_{k+1}}^{t_k + T_p} g_i(\bar{\mathbf{e}}_i(s; \mathbf{e}_i(t_{k+1})), \bar{\mathbf{u}}_i^*(s)) ds$, and $\bar{\mathbf{e}}_i(t_k + T_p; \bar{\mathbf{u}}_i^*(\cdot, \mathbf{e}_i(t_k))) = \bar{\mathbf{e}}_i(t_{k+1}) + \int_{t_{k+1}}^{t_k + T_p} g_i(\bar{\mathbf{e}}_i(s; \mathbf{e}_i(t_k)), \bar{\mathbf{u}}_i^*(s)) ds$. Subtracting the latter from the former and taking norms on both sides we get: $\left\| \bar{\mathbf{e}}_i(t_k + T_p; \bar{\mathbf{u}}_i^*(\cdot, \mathbf{e}_i(t_{k+1}))) - \bar{\mathbf{e}}_i(t_k + T_p; \bar{\mathbf{u}}_i^*(\cdot, \mathbf{e}_i(t_k))) \right\| \leq \left\| \mathbf{e}_i(t_{k+1}) - \bar{\mathbf{e}}_i(t_{k+1}) \right\| + L_{g_i} \int_h^{T_p} \left\| \bar{\mathbf{e}}_i(t_k + s; \bar{\mathbf{u}}_i^*(\cdot, \mathbf{e}_i(t_{k+1}))) - \bar{\mathbf{e}}_i(t_k + s; \bar{\mathbf{u}}_i^*(\cdot, \mathbf{e}_i(t_k))) \right\| ds$. By applying the Grönwall-Bellman inequality we obtain: $\left\| \bar{\mathbf{e}}_i(t_k + T_p; \bar{\mathbf{u}}_i^*(\cdot, \mathbf{e}_i(t_{k+1}))) - \bar{\mathbf{e}}_i(t_k + T_p; \bar{\mathbf{u}}_i^*(\cdot, \mathbf{e}_i(t_k))) \right\| \leq \left\| \mathbf{e}_i(t_{k+1}) - \bar{\mathbf{e}}_i(t_{k+1}) \right\|$

¹ $A = B_1 \oplus B_2 \Rightarrow A \ominus B = (A \ominus B_1) \ominus B_2$

² $(A \oplus B) \ominus B \subseteq A$

$-\bar{\mathbf{e}}_i(t_{k+1})\Big\|e^{L_{g_i}(T_p-h)}$. By applying Lemma 3 for $t = t_k$ and $\tau = h$ we have:
 $\left\|\bar{\mathbf{e}}_i(t_k + T_p; \bar{\mathbf{u}}_i^*(\cdot), \mathbf{e}_i(t_{k+1})) - \bar{\mathbf{e}}_i(t_k + T_p; \bar{\mathbf{u}}_i^*(\cdot), \mathbf{e}_i(t_k))\right\| \leq \frac{\bar{w}_i}{L_{g_i}}(e^{L_{g_i}h} - 1)e^{L_{g_i}(T_p-h)}$.
Hence (H5) becomes:

$$\begin{aligned} V_i(\bar{\mathbf{e}}_i(t_k + T_p; \bar{\mathbf{u}}_i^*(\cdot), \mathbf{e}_i(t_{k+1}))) - V_i(\bar{\mathbf{e}}_i(t_k + T_p; \bar{\mathbf{u}}_i^*(\cdot), \mathbf{e}_i(t_k))) \\ = L_{V_i} \frac{\bar{w}_i}{L_{g_i}}(e^{L_{g_i}h} - 1)e^{L_{g_i}(T_p-h)}. \end{aligned} \quad (\text{H6})$$

Since the solution to the optimization problem is assumed to be feasible at time t_k , all states fulfill their respective constraints, and in particular, from (H2), the predicted state $\bar{\mathbf{e}}_i(t_k + T_p; \bar{\mathbf{u}}_i^*(\cdot), \mathbf{e}_i(t_k)) \in \Omega_i$. This means that $V_i(\bar{\mathbf{e}}_i(t_k + T_p; \bar{\mathbf{u}}_i^*(\cdot), \mathbf{e}_i(t_k))) \leq \varepsilon_{\Omega_i}$. Hence (H6) becomes: $V_i(\bar{\mathbf{e}}_i(t_k + T_p; \bar{\mathbf{u}}_i^*(\cdot), \mathbf{e}_i(t_{k+1}))) \leq \varepsilon_{\Omega_i} + L_{V_i} \frac{\bar{w}_i}{L_{g_i}}(e^{L_{g_i}h} - 1)e^{L_{g_i}(T_p-h)}$. From Assumption 4 of Theorem 1, the upper bound

of the disturbance is in turn bounded by: $\bar{w}_i \leq \frac{\varepsilon_{\Psi_i} - \varepsilon_{\Omega_i}}{\frac{L_{V_i}}{L_{g_i}}(e^{L_{g_i}h} - 1)e^{L_{g_i}(T_p-h)}}$. Therefore:

$V_i(\bar{\mathbf{e}}_i(t_k + T_p; \bar{\mathbf{u}}_i^*(\cdot), \mathbf{e}_i(t_{k+1}))) \leq \varepsilon_{\Psi_i}$, or, expressing the above in terms of t_{k+1} instead of t_k : $V_i(\bar{\mathbf{e}}_i(t_{k+1} + T_p - h; \bar{\mathbf{u}}_i^*(\cdot), \mathbf{e}_i(t_{k+1}))) \leq \varepsilon_{\Psi_i}$. This means that the state $\bar{\mathbf{e}}_i(t_{k+1} + T_p - h; \bar{\mathbf{u}}_i^*(\cdot), \mathbf{e}_i(t_{k+1})) \in \Psi_i$. From Assumption 7, and since $\Psi_i \subseteq \Phi_i$, there is an admissible control signal $\kappa_i(\bar{\mathbf{e}}_i(t_{k+1} + T_p - h; \bar{\mathbf{u}}_i^*(\cdot), \mathbf{e}_i(t_{k+1})))$ such that: $\bar{\mathbf{e}}_i(t_{k+1} + T_p; \kappa_i(\cdot), \bar{\mathbf{e}}_i(t_{k+1} + T_p - h; \bar{\mathbf{u}}_i^*(\cdot), \mathbf{e}_i(t_{k+1}))) \in \Omega_i$. Hence, overall, it holds that:

$$\bar{\mathbf{e}}_i(t_{k+1} + T_p; \tilde{\mathbf{u}}_i(\cdot), \mathbf{e}_i(t_{k+1})) \in \Omega_i. \quad (\text{H7})$$

Piecing the admissibility of $\tilde{\mathbf{u}}_i(\cdot)$ from (H3) together with conclusions (H4) and (H7), we conclude that the application of the control input $\tilde{\mathbf{u}}_i(\cdot)$ at time t_{k+1} results in that the states of the real system fulfill their intended constraints during the entire horizon $[t_{k+1}, t_{k+1} + T_p]$. Therefore, overall, the (sub-optimal) control input $\tilde{\mathbf{u}}_i(\cdot)$ is admissible at time t_{k+1} according to Definition 7, which means that feasibility of a solution to the optimization problem at time t_k implies feasibility at time $t_{k+1} > t_k$. Thus, since at time $t = 0$ a solution is assumed to be feasible, a solution to the optimal control problem is feasible for all $t \geq 0$. \square

Appendix I. Convergence Analysis

The second part of the proof involves demonstrating that the state \mathbf{e}_i is ultimately bounded in Ω_i . We will show that the *optimal* cost $J_i^*(\mathbf{e}_i(t))$ is an ISS Lyapunov function for the closed loop system (6), under the control input (11), where: $J_i^*(\mathbf{e}_i(t)) \triangleq J_i(\mathbf{e}_i(t), \bar{\mathbf{u}}_i^*(\cdot; \mathbf{e}_i(t)))$. For notational convenience, let us as define the following terms:

- $\mathbf{u}_{0,i}(\tau) \triangleq \bar{\mathbf{u}}_i^*(\tau; \mathbf{e}_i(t_k))$ as the *optimal* input that results from the solution to Problem 1 based on the measurement of state $\mathbf{e}_i(t_k)$, applied at time $\tau \geq t_k$;
- $\mathbf{e}_{0,i}(\tau) \triangleq \bar{\mathbf{e}}_i(\tau; \bar{\mathbf{u}}_i^*(\cdot; \mathbf{e}_i(t_k)), \mathbf{e}_i(t_k))$ as the *predicted* state at time $\tau \geq t_k$,

that is, the predicted state that results from the application of the above input $\bar{\mathbf{u}}_i^*(\cdot; \mathbf{e}_i(t_k))$ to the state $\mathbf{e}_i(t_k)$, at time τ ;

- $\mathbf{u}_{1,i}(\tau) \triangleq \tilde{\mathbf{u}}_i(\tau)$ as the *admissible* input at $\tau \geq t_{k+1}$ (see (H3));
- $\mathbf{e}_{1,i}(\tau) \triangleq \bar{\mathbf{e}}_i(\tau; \tilde{\mathbf{u}}_i(\cdot), \mathbf{e}_i(t_{k+1}))$ as the *predicted* state at time $\tau \geq t_{k+1}$, that is, the predicted state that results from the application of the above input $\tilde{\mathbf{u}}_i(\cdot)$ to the state $\mathbf{e}_i(t_{k+1}; \bar{\mathbf{u}}_i^*(\cdot; \mathbf{e}_i(t_k)), \mathbf{e}_i(t_k))$, at time τ .

Before beginning to prove convergence, it is worth noting that while the cost $J_i(\mathbf{e}_i(t), \bar{\mathbf{u}}_i^*(\cdot; \mathbf{e}_i(t)))$, is optimal (in the sense that it is based on the optimal input, which provides its minimum realization), a cost that is based on a plainly admissible (and thus, without loss of generality, sub-optimal) input $\mathbf{u}_i \neq \bar{\mathbf{u}}_i^*$ will result in a configuration where: $J_i(\mathbf{e}_i(t), \mathbf{u}_i(\cdot; \mathbf{e}_i(t))) \geq J_i(\mathbf{e}_i(t), \bar{\mathbf{u}}_i^*(\cdot; \mathbf{e}_i(t)))$.

Let us now begin our investigation on the sign of the difference between the cost that results from the application of the feasible input $\mathbf{u}_{1,i}$, which we shall denote by $\bar{J}_i(\mathbf{e}_i(t_{k+1}))$, and the optimal cost $J_i^*(\mathbf{e}_i(t_k))$, while recalling that: $J_i(\mathbf{e}_i(t), \bar{\mathbf{u}}_i(\cdot)) = \int_t^{t+T_p} F_i(\bar{\mathbf{e}}_i(s), \bar{\mathbf{u}}_i(s)) ds + V_i(\bar{\mathbf{e}}_i(t + T_p))$:

$$\begin{aligned} \bar{J}_i(\mathbf{e}_i(t_{k+1})) - J_i^*(\mathbf{e}_i(t_k)) &= V_i(\mathbf{e}_{1,i}(t_{k+1} + T_p)) + \int_{t_{k+1}}^{t_{k+1}+T_p} F_i(\mathbf{e}_{1,i}(s), \mathbf{u}_{1,i}(s)) ds \\ &\quad - V_i(\mathbf{e}_{0,i}(t_k + T_p)) - \int_{t_k}^{t_k+T_p} F_i(\mathbf{e}_{0,i}(s), \mathbf{u}_{0,i}(s)) ds. \end{aligned} \quad (I1)$$

Considering that $t_k < t_{k+1} < t_k + T_p < t_{k+1} + T_p$, we break down the two integrals above in between these integrals:

$$\begin{aligned} \bar{J}_i(\mathbf{e}_i(t_{k+1})) - J_i^*(\mathbf{e}_i(t_k)) &= \\ &V_i(\mathbf{e}_{1,i}(t_{k+1} + T_p)) + \int_{t_{k+1}}^{t_k+T_p} F_i(\mathbf{e}_{1,i}(s), \mathbf{u}_{1,i}(s)) ds + \int_{t_k+T_p}^{t_{k+1}+T_p} F_i(\mathbf{e}_{1,i}(s), \mathbf{u}_{1,i}(s)) ds \\ &- V_i(\mathbf{e}_{0,i}(t_k + T_p)) - \int_{t_k}^{t_{k+1}} F_i(\mathbf{e}_{0,i}(s), \mathbf{u}_{0,i}(s)) ds - \int_{t_{k+1}}^{t_k+T_p} F_i(\mathbf{e}_{0,i}(s), \mathbf{u}_{0,i}(s)) ds. \end{aligned} \quad (I2)$$

Let us first focus on the difference between the two intervals in (I2) over $[t_{k+1}, t_{k+1}+T_p]$:

$$\begin{aligned} &\int_{t_{k+1}}^{t_k+T_p} F_i(\mathbf{e}_{1,i}(s), \mathbf{u}_{1,i}(s)) ds - \int_{t_{k+1}}^{t_k+T_p} F_i(\mathbf{e}_{0,i}(s), \mathbf{u}_{0,i}(s)) ds \\ &\leq \left| \int_{t_k+h}^{t_k+T_p} F_i(\mathbf{e}_{1,i}(s), \mathbf{u}_{1,i}(s)) ds - \int_{t_k+h}^{t_k+T_p} F_i(\mathbf{e}_{0,i}(s), \mathbf{u}_{0,i}(s)) ds \right| \\ &\leq L_{F_i} \int_h^{T_p} \left\| \bar{\mathbf{e}}_i(t_k + s; \bar{\mathbf{u}}_i^*(\cdot), \mathbf{e}_i(t_k + h)) - \bar{\mathbf{e}}_i(t_k + s; \bar{\mathbf{u}}_i^*(\cdot), \mathbf{e}_i(t_k)) \right\| ds. \end{aligned} \quad (I3)$$

Consulting with Remark 3 for the two different initial conditions we get: $\bar{\mathbf{e}}_i(t_k + s; \bar{\mathbf{u}}_i^*(\cdot), \mathbf{e}_i(t_k + h)) = \mathbf{e}_i(t_k + h) + \int_{t_k+h}^{t_k+s} g_i(\bar{\mathbf{e}}_i(\tau; \mathbf{e}_i(t_k + h)), \bar{\mathbf{u}}_i^*(\tau)) d\tau$, and $\bar{\mathbf{e}}_i(t_k + s; \bar{\mathbf{u}}_i^*(\cdot), \mathbf{e}_i(t_k)) = \mathbf{e}_i(t_k) + \int_{t_k}^{t_k+h} g_i(\bar{\mathbf{e}}_i(\tau; \mathbf{e}_i(t_k)), \bar{\mathbf{u}}_i^*(\tau)) d\tau + \int_{t_k+h}^{t_k+s} g_i(\bar{\mathbf{e}}_i(\tau; \mathbf{e}_i(t_k)), \bar{\mathbf{u}}_i^*(\tau)) d\tau$. Subtracting the latter from the former and taking

norms on either side yields:

$$\begin{aligned} & \left\| \bar{\mathbf{e}}_i(t_k + s; \bar{\mathbf{u}}_i^*(\cdot), \mathbf{e}_i(t_k + h)) - \bar{\mathbf{e}}_i(t_k + s; \bar{\mathbf{u}}_i^*(\cdot), \mathbf{e}_i(t_k)) \right\| \leq \left\| \mathbf{e}_i(t_k + h) - \bar{\mathbf{e}}_i(t_k + h) \right\| \\ & + L_{g_i} \int_h^s \left\| \bar{\mathbf{e}}_i(t_k + \tau; \bar{\mathbf{u}}_i^*(\cdot), \mathbf{e}_i(t_k + h)) - \bar{\mathbf{e}}_i(t_k + \tau; \bar{\mathbf{u}}_i^*(\cdot), \mathbf{e}_i(t_k)) \right\| d\tau. \end{aligned} \quad (I4)$$

By using Lemma 3 and applying the the Grönwall-Bellman inequality, (I4) becomes:

$$\left\| \bar{\mathbf{e}}_i(t_k + s; \bar{\mathbf{u}}_i^*(\cdot), \mathbf{e}_i(t_k + h)) - \bar{\mathbf{e}}_i(t_k + s; \bar{\mathbf{u}}_i^*(\cdot), \mathbf{e}_i(t_k)) \right\| \leq \frac{\bar{w}_i}{L_{g_i}} (e^{L_{g_i} h} - 1) e^{L_{g_i}(s-h)}.$$

Given the above result, (I3) becomes:

$$\begin{aligned} & \int_{t_{k+1}}^{t_k + T_p} F_i(\mathbf{e}_{1,i}(s), \mathbf{u}_{1,i}(s)) ds - \int_{t_{k+1}}^{t_k + T_p} F_i(\mathbf{e}_{0,i}(s), \mathbf{u}_{0,i}(s)) ds \\ & \leq L_{F_i} \frac{\bar{w}_i}{L_{g_i}^2} (e^{L_{g_i} h} - 1) (e^{L_{g_i}(T_p-h)} - 1). \end{aligned} \quad (I5)$$

With this result established, we turn back to the remaining terms found in (I2) and, in particular, we focus on the integral: $\int_{t_k + T_p}^{t_{k+1} + T_p} F_i(\mathbf{e}_{1,i}(s), \mathbf{u}_{1,i}(s)) ds$. We discern that the range of this integral has a length equal to the length of the interval where (I4) of Assumption 6 holds. Integrating (I4) over the interval $[t_k + T_p, t_{k+1} + T_p]$,

$$\begin{aligned} & \text{for the controls and states applicable in it we get: } \int_{t_k + T_p}^{t_{k+1} + T_p} \left(\frac{\partial V_i}{\partial \mathbf{e}_{1,i}} g_i(\mathbf{e}_{1,i}(s), \mathbf{u}_{1,i}(s)) \right. \\ & \left. + F_i(\mathbf{e}_{1,i}(s), \mathbf{u}_{1,i}(s)) \right) ds \leq 0 \Leftrightarrow V_i(\mathbf{e}_{1,i}(t_{k+1} + T_p)) + \int_{t_k + T_p}^{t_{k+1} + T_p} F_i(\mathbf{e}_{1,i}(s), \mathbf{u}_{1,i}(s)) ds \\ & \leq V_i(\mathbf{e}_{1,i}(t_k + T_p)). \text{ The left-hand side expression is the same as the first two terms in} \\ & \text{the right-hand side of equality (I2). We can introduce the third one by subtracting it} \\ & \text{from both sides: } V_i(\mathbf{e}_{1,i}(t_{k+1} + T_p)) + \int_{t_k + T_p}^{t_{k+1} + T_p} F_i(\mathbf{e}_{1,i}(s), \mathbf{u}_{1,i}(s)) ds - V_i(\mathbf{e}_{0,i}(t_k + T_p)) \\ & \leq L_{V_i} \frac{\bar{w}_i}{L_{g_i}} (e^{L_{g_i} h} - 1) e^{L_{g_i}(T_p-h)}. \text{ Hence, we obtain:} \end{aligned}$$

$$\begin{aligned} & V_i(\mathbf{e}_{1,i}(t_{k+1} + T_p)) + \int_{t_k + T_p}^{t_{k+1} + T_p} F_i(\mathbf{e}_{1,i}(s), \mathbf{u}_{1,i}(s)) ds - V_i(\mathbf{e}_{0,i}(t_k + T_p)) \\ & \leq L_{V_i} \frac{\bar{w}_i}{L_{g_i}} (e^{L_{g_i} h} - 1) e^{L_{g_i}(T_p-h)}. \end{aligned} \quad (I6)$$

Adding the inequalities (I5) and (I6) it is derived that: $\int_{t_{k+1}}^{t_k + T_p} F_i(\mathbf{e}_{1,i}(s), \mathbf{u}_{1,i}(s)) ds - \int_{t_{k+1}}^{t_k + T_p} F_i(\mathbf{e}_{0,i}(s), \mathbf{u}_{0,i}(s)) ds + V_i(\mathbf{e}_{1,i}(t_{k+1} + T_p)) + \int_{t_k + T_p}^{t_{k+1} + T_p} F_i(\mathbf{e}_{1,i}(s), \mathbf{u}_{1,i}(s)) ds - V_i(\mathbf{e}_{0,i}(t_k + T_p)) \leq L_{F_i} \frac{\bar{w}_i}{L_{g_i}^2} (e^{L_{g_i} h} - 1) (e^{L_{g_i}(T_p-h)} - 1) + L_{V_i} \frac{\bar{w}_i}{L_{g_i}} (e^{L_{g_i} h} - 1) e^{L_{g_i}(T_p-h)}$,

and therefore (I2), by bringing the integral ranging from t_k to t_{k+1} to the left-hand side, becomes: $\bar{J}_i(\mathbf{e}_i(t_{k+1})) - J_i^*(\mathbf{e}_i(t_k)) + \int_{t_k}^{t_{k+1}} F_i(\mathbf{e}_{0,i}(s), \mathbf{u}_{0,i}(s)) ds \leq L_{F_i} \frac{\bar{w}_i}{L_{g_i}^2} (e^{L_{g_i} h} - 1) (e^{L_{g_i}(T_p-h)} - 1) + L_{V_i} \frac{\bar{w}_i}{L_{g_i}} (e^{L_{g_i} h} - 1) e^{L_{g_i}(T_p-h)}$. By rearranging terms, the cost difference becomes bounded by: $\bar{J}_i(\mathbf{e}_i(t_{k+1})) - J_i^*(\mathbf{e}_i(t_k)) \leq \xi_i \bar{w}_i$

$-\int_{t_k}^{t_{k+1}} F_i(\mathbf{e}_{0,i}(s), \mathbf{u}_{0,i}(s)) ds$, where: $\xi_i \triangleq \frac{1}{L_{g_i}} \left(e^{L_{g_i} h} - 1 \right) \left[(L_{V_i} + \frac{L_{F_i}}{L_{g_i}}) (e^{L_{g_i}(T_p-h)} - 1) + L_{V_i} \right] > 0$, and $\xi_i \bar{w}_i$ is the contribution of the bounded additive disturbance $\mathbf{w}_i(t)$ to the nominal cost difference; F_i is a positive-definite function as a sum of a positive-definite $\mathbf{u}_i^\top \mathbf{R}_i \mathbf{u}_i$ and a positive semi-definite function $\mathbf{e}_i^\top \mathbf{Q}_i \mathbf{e}_i$. If we denote by $m_i \triangleq \lambda_{\min}(\mathbf{Q}_i, \mathbf{R}_i) \geq 0$ the minimum eigenvalue between those of matrices $\mathbf{R}_i, \mathbf{Q}_i$, this means that: $F_i(\mathbf{e}_{0,i}(s), \mathbf{u}_{0,i}(s)) \geq m_i \|\mathbf{e}_{0,i}(s)\|^2$. By integrating the above between the interval of interest $[t_k, t_{k+1}]$ we get: $-\int_{t_k}^{t_{k+1}} F_i(\mathbf{e}_{0,i}(s), \mathbf{u}_{0,i}(s)) \leq -m_i \int_{t_k}^{t_{k+1}} \|\bar{\mathbf{e}}_i(s; \bar{\mathbf{u}}_i^*, \mathbf{e}_i(t_k))\|^2 ds$. This means that the cost difference is upper-bounded by: $\bar{J}_i(\mathbf{e}_i(t_{k+1})) - J_i^*(\mathbf{e}_i(t_k)) \leq \xi_i \bar{w}_i - m_i \int_{t_k}^{t_{k+1}} \|\bar{\mathbf{e}}_i(s; \bar{\mathbf{u}}_i^*(\cdot), \mathbf{e}_i(t_k))\|^2 ds$, and since the cost $\bar{J}_i(\mathbf{e}_i(t_{k+1}))$ is, in general, sub-optimal: $J_i^*(\mathbf{e}_i(t_{k+1})) - \bar{J}_i(\mathbf{e}_i(t_{k+1})) \leq 0$: $J_i^*(\mathbf{e}_i(t_{k+1})) - J_i^*(\mathbf{e}_i(t_k)) \leq \xi_i \bar{w}_i - m_i \int_{t_k}^{t_{k+1}} \|\bar{\mathbf{e}}_i(s; \bar{\mathbf{u}}_i^*(\cdot), \mathbf{e}_i(t_k))\|^2 ds$. Let $\Xi_i(\mathbf{e}_i) \triangleq J_i^*(\mathbf{e}_i)$. Then, between consecutive times t_k and t_{k+1} when the FHOCP is solved, the last inequality reforms into:

$$\Xi_i(\mathbf{e}_i(t_{k+1})) - \Xi_i(\mathbf{e}_i(t_k)) \leq \int_{t_k}^{t_{k+1}} \left(\frac{\xi_i}{h} \|\mathbf{w}_i(s)\| - m_i \|\bar{\mathbf{e}}_i(s; \bar{\mathbf{u}}_i^*(\cdot), \mathbf{e}_i(t_k))\|^2 \right) ds. \quad (\text{I7})$$

The functions $\sigma(\|\mathbf{w}_i\|) \triangleq \frac{\xi_i}{h} \|\mathbf{w}_i\|$ and $\alpha_3(\|\mathbf{e}_i\|) \triangleq m_i \|\mathbf{e}_i\|^2$ are class \mathcal{K} functions, and therefore, according to Lemma 4, $\Xi_i(\mathbf{e}_i)$ is an ISS Lyapunov function in \mathcal{E}_i . Given this fact, the closed-loop system is input-to-state stable in \mathcal{E}_i . Inevitably then, given Assumptions 6 and 7, and condition (3) of Theorem 1, the closed-loop trajectories for the error state of agent $i \in \mathcal{V}$ reach the terminal set Ω_i for all $\mathbf{w}_i(t)$ with $\|\mathbf{w}_i(t)\| \leq \bar{w}_i$, at some point $t = t^* \geq 0$. Once inside Ω_i , the trajectory is trapped there because of the implications³ of (I7) and Assumption 7.

In turn, this means that the system (6) converges to $\mathbf{z}_{i,\text{des}}$ and is trapped in a vicinity of it – smaller than that in which it would have been trapped (if actively trapped at all) in the case of unattenuated disturbances –, while simultaneously conforming to all constraints \mathcal{Z}_i . This conclusion holds for all $i \in \mathcal{V}$, and hence, the overall system of agents \mathcal{V} is stable. \square

³For more details, refer to the discussion after the declaration of Theorem 7.6 in [35].